WILEY-VCH

DOI: 10.1002/((please add manuscript number))
Article type: Full Paper

Title: Non-invasive featherlight wearable compliant "Marine Skin" – standalone multi-sensory system for deep-sea environmental monitoring

*Sohail F. Shaikh[1], Harold F. Mazo-Mantilla[1], Nadeem Qaiser[1], Sherjeel M. Khan[1], Joanna M. Nassar[2], Nathan R. Geraldi[3], Carlos M. Duarte[3], and Muhammad M. Hussain[1]**

[1]mmh Labs, Electrical Engineering, Computer Electrical Mathematical Science and Engineering Division (CEMSE), King Abdullah University of Science and Technology (KAUST), Thuwal 23955-6900, Saudi Arabia
[2]California Institute of Technology, Pasadena, CA 91125, USA.
[3]Red Sea Research Center (RSRC), Division of Biological and Environmental Sciences and Engineering (BESE), King Abdullah University of Science and Technology (KAUST), Thuwal 23955-6900, Saudi Arabia

*Corresponding author's e-mail: muhammadmustafa.hussain@kaust.edu.sa

Keywords: marine ecology; flexible sensors; non-invasive tag; soft packaging; hybrid integration.

Abstract

Advances in the marine research to understand the environmental change and its effect on marine ecosystems rely on gathering data on species physiology, their habitat, and their mobility patterns using heavy and invasive biologgers and sensory telemetric networks. In the past, we have demonstrated lightweight (6 grams) compliant environmental monitoring system: "Marine Skin". In this paper, we report an enhanced version of that skin with improved functionalities (500-1500% enhanced sensitivity), packaging and the most importantly its endurance at a depth of 2 km in the highly saline Red Sea water for 4 consecutive weeks. We also illustrate a unique non-invasive approach for attachment of the sensor by designing a wearable, stretchable jacket (bracelet) that can adhere to any species irrespective of their skin type. We deployed the wearable feather-light (<0.5g in air, 3g with jacket) gadget on Barramundi, Seabream, and common Goldfish to

demonstrate the non-invasive and effective attachment strategy on different species of variable sizes which does not hinder the animals' natural movement or behavior.

1. INTRODUCTION

The marine environment - a continuous provider of valuable goods and services for decades, has been directly or indirectly altered by extensive human impacts. Direct harvesting, rigorous over-exploitation by fisheries, run-off of nutrients and pollutants, and pollution contribute to the anthropogenic changes occurring in the oceanic ecosystem. [1] The impact of the human activities on the marine ecosystem varies with the intensity of resources extraction, pollutant addition, and the changes in the species composition. It is estimated that 41% of the oceans are impacted by multiple activities. [2] To facilitate the policy implementations, trade-offs and devise mitigation strategies at global scales, it is of utmost importance to quantify and map environmental variables and human activities throughout the marine environment. [2–5] Recent developments in the electronic tagging devices and animal-borne bio-loggers have facilitated quantifying ecosystems and the effect of humans. Animal-borne tagging devices are used to understand the animal migration (plasticity of dates and routes, and mechanisms), foraging behavior, physiological performances, habitat selection, and social interaction with other species, as well as abiotic environmental variables. [6,7] To maintain the physiology, normal behavior, and the survival of tagged animals, the weight of the electronic tag should not exceed 2% of the body weight. [8–10] Most of the available CTD (conductivity, temperature, and depth) bio-logging devices fail to adhere to the 2% weight regime, in addition, they are rigid, bulky, and expensive, not suitable for the smaller species, young specimens, and invertebrates. [11,12] Invasive methods of attachment, as well as bulky and expensive devices have restricted the focus of studies to larger species such as dolphins, sirenians, sharks, and cetaceans. Commonly adopted practices for the attachment of

devices use a crossbow or a shotgun to insert the device in the tissue of the species. Incisions and surgical tools and/or mechanical bolts are frequently used for fixation of the tags to the fins of the animals. [13–15] However, these attachment methodologies fail to sustain extended periods underwater due to the drag forces and behavior of the marine species (both tagged and surrounding). Studies have revealed the serious repercussion of the weight and design of the tag, and the invasive attachment methods which influence diving patterns, swimming, foraging, mating and nesting behaviors. [16–19]

Despite the technological advancements in the marine tagging electronic devices (e.g. CTD), the majority of limitations related to animal comfort, non-invasive attachment, and adaptability to the myriad of aquatic species (from a tiny goldfish to large mammals) remain unaddressed. In addition, prolonged lifetime of the tag increased sensing capabilities, and conformal (flexible) design of the devices that do not influence the natural behavior of animals, present another level of challenges. Addressing the reliability of performance under any mechanical deformation, extreme pressures and complex behavior after extended submersion in seawater without any biofouling is also important. Therefore, there is an urgent need to focus efforts toward making marine electronic tagging systems that are lightweight, conformal, and that does not exceed the cost of currently available sensors. Moreover, the packaging should be biocompatible, robust, leak-proof, and reliable for sustained underwater exposure. The tag must be non-invasively capable of monitoring the marine environment even at great depths, without hindering the current status-quo in terms of resolution and high performance while having a simple attachment mechanism.

Convolution of state-of-the-art complementary metal oxide semiconductor (CMOS) technologies, materials, and advances in the field of flexible electronics is driving the technologies of the future, where data, processes, sensors, and living and non-living things interact in synergy

for the Internet of Everything (IoE) applications. [20–23] Recently, we demonstrated "Marine-Skin"- a lightweight non-invasive physically flexible skin-like multifunctional electronic tagging system with waterproof packaging [6]. The Marine-Skin tagging system was lighter (~6 g in air) than ever reported previously, conformal with a biocompatible packaging and a non-invasive tagging method never reported before. The resolution and the accuracies of the sensory system were not compromised after deployment or from the physical deformations when attached to the hard-shell crustaceans using glue. That Marine-Skin system was tested in a controlled environment in the lab for different measurements where the maximum depth of water was < 80 cm. In addition, the deployment on crustaceans demonstrated the real-time acquisition of data at shallow water depths (<60 cm). The majority of the small fishes, many sharks, dolphins, and other species primarily inhabit the ocean's surface (<200 m depth), but also dive deeper than 600 m in search of a prey and routine behavior. Consequently, it is the necessity to have sensors that withstand the pressure of water at great depths (at least within 600 m). Furthermore, the attachment method used previously (super-glue or waterproof adhesive) only works on animals with exoskeletons or shells such as crustaceans or sea turtle.

Considering these challenges and issues faced during deployment of the first version of Marine-Skin, we are presenting an advanced and improved version of Marine-Skin platform that is lighter than the previous version, smaller (halved), flexible, and has a robust biocompatible packaging for dramatically reducing the biofouling after deployment over extended periods. We report drastic improvements in the performance by optimizing the materials and modifying the design. We demonstrate for the first time sustained performance in extremely harsh environments with high-pressure (~3000 psi, up to 2 km depth), prolonged exposure to highly saline Red Sea water (~ 1 month, ~41 PSU), and extreme bending cycles (10000 cycles, bending radius of 2 mm).

In addition, we demonstrate a pragmatic non-invasive attachment technique in the form of unique bracelet-like jacket designs for extreme animal comfort without influencing the natural movement of tagged individuals. This unique wearable jacket design will be suitable for tagging most of the marine species irrespective of their skin type without any need of glue or incisions. **Figure 1** represents the basic concept of Marine-Skin with a wearable soft jacket gadget design that can monitor the microenvironment with varying extreme oceanic conditions of pressure, temperature, and salinity. Furthermore, the electronic tagging platform that can withstand harsh environments with high-pressure, high salinity, and reduced temperatures, can further strengthen the quest of exploring, studying, and protecting deep-sea ecosystems (> 1000 m depth), which cover more than 50% of the earth's surface but remains poorly studied.

2. RESULTS AND DISCUSSION

Conventionally, CTD based tagging systems have been used to monitor three fundamental parameters (conductivity, temperature, and depth) of the marine environment to understand the composition, water masses and the niche used by marine life. [24] There still exists major challenges for developing marine sensors, including underwater data acquisition. There are huge efforts to develop reliable underwater communication including acoustic and optical communication. Optical communication underwater presents a lot of promise to solve this persistent challenge, however, these technologies are in their infancy. [25–28] Thus, an alternative approach is to store the data in the memory embedded on the platform and transfer the stored data when the animal comes to the surface of the water during its natural behavior. Hueter *et al.* recently demonstrated the usage of a satellite-linked MiniPAT^{TM} system for tracking the movement of *Carcharhinus falciformis* (silky shark) to understand the ecology of this large, oceanic species. [29] The attachment method

consisted of inserting a plastic or stainless steel anchor into the skin, which is not only invasive but also discomforting to the animal. Moreover, the device is not attached to the animal's body but is hanging with a support, which can be harmful during movement and can be detached (break).

In our Marine-Skin system, we integrated the Bluetooth system on a chip (SoC) and a memory module with a small battery, which was encapsulated in a waterproof and biocompatible packaging. Great efforts were taken to make the system flexible, stretchable, and featherlight, which can be attached non-invasively using a wearable soft jacket architecture. The SoC and memory module stores the acquired data underwater and can be retrieved from memory after the tag is retrieved by connecting it to a Bluetooth enabled device. The flexible, small, and lightweight platform combined with the wearable jacket design resulted in a sensor with minimal discomfort to any tagged species irrespective of their size or epidermal type.

2.1. *Biocompatible Soft Packaging*

Any sensory platform designed for the marine environment must retain its performance under high salinity, high pressure and this corrosive aqueous environment. The salinity of the sea water varies in different geographical locations; nevertheless, it can range from 35-40 practical salinity unit (PSU). [30,31] Therefore, the first challenge in the "Marine Skin" tagging development was to have a compliant packaging material that is soft to adhere to the animal's skin, elastic to maintain the stretchability (for comfortable breathing and comply with physical deformation) of the device. Different material choices available for such soft encapsulation are Ecoflex©, and polymethyl methyl acrylate (PMMA), and polydimethylsiloxane (PDMS). We chose polydimethylsiloxane (PDMS) (Sylgard 184^{TM}) as the soft encapsulation of the sensory platform due to its hydrophobic, non-toxic, non-decomposing, and non-irritating properties. In comparison, Ecoflex undergoes biodegradation and PDMS does not decompose or undergo major polymeric deformations when

exposed to certain kind of microorganism found in seawater. [32–34] Further, PDMS is one of the most used materials in microfluidics and biosensors because of its biocompatibility. In addition, PDMS has a hydrophobic surface having lower surface energy. This low surface energy provides a weaker adhesion of the biofouling layer on the PDMS surface. A textured PDMS surface has been also reported to provide a weaker adhesion of biofouling elements thus making it easier to shrug off after a simple rinsing process. [34–36] To study the biofouling effects on the PDMS encapsulated devices, we immersed the samples for 6 weeks in the Red seawater. The samples were retrieved and then scanning electron microscopic images were captured to analyze the surface **Figure S8a and S8b**. The blank surface of PDMS shows some textured surface which is known to help in rinsing off the developed biofouling easily. We have observed salt accumulation and a few diatoms (Figure S8b inset), however, we have not observed any live organism under the fluorescence microscope. We later performed O_2 plasma on the PDMS surface which gave more pronounced texture visible in Figure S8c and this textured PDMS has reduced biofouling significantly as can be noticed in Figure S8d. In addition, the hydrophobicity, low surface-energy, and the textured surface of the PDMS provide an extremely low adhesion of the biofouling that can be rinsed/washed off due to the drag forces within the water and the residues can be further removed by the rinsing process.

2.2. Multisensory Compliant Design

"Marine Skin" is a stretchable and flexible multisensory platform that monitors temperature, pressure (depth), and the salinity of the marine environment. The pressure sensor is based on an array of multiple pixels of capacitors all connected in parallel. If the end electrodes are not connected, the pressure at individual pixels can be mapped. We use PDMS as a soft and compressible dielectric material for the capacitive pressure sensors. The sinusoidal wavy

architecture of metallic interconnects allow the stretchability in lateral directions while also maintaining the twisting and bending capability due to inherent soft elastic properties of PDMS encapsulating material. [37,38] A resistive temperature detector (RTD) is fabricated for temperature measurements while the salinity sensor was incorporated by using an interdigitated electrode architecture for enhancing the sensitivity. The miniaturized version 2 measures 20 mm × 20 mm × 0.3 mm.

Currently available electronic products in the market for marine animal tagging are rigid, with packaging in a stiff acrylic or plastic package. The core of the tag is a printed circuit board (PCB) that hosts different components and the sensor integrated circuit (ICs). Having all the rigid ICs with passive electronic components (resistors and capacitors) soldered on the rigid PCB, no matter how small, will not make a system flexible. There are many groups that focus on polymeric materials for using it as a flexible substrate in flexible electronics. It must be noted that merely changing the substrate from PCB and mounting the same rigid ICs on the flexible PCB does not make it flexible for the desired application. Moreover, many presented flexible systems have flexible sensory parts but the core of the readout circuit is a microcontroller or data acquisition system that in itself is not flexible, also, the sensory platforms are not stand-alone. [39–41] Most often, these flexible sensors are connected to the data acquisition system by either wire-bonding or soldering wired connectors that again makes the system vulnerable for failure. Hence, a practical approach towards obtaining a fully compliant system needs absolutely no rigid components. This can be achieved if we can integrate the unpacked (bare die) version of the ICs required in the system and make them flexible.

Here we present a complete integration strategy for the multisensory “Marine Skin” platform and the system is detailed in 3D schematic flow presented in **Figure 2**. This integration flow is

devised considering into account the low-cost CMOS fabrication approach, scalability, high-yield, batch fabrication, and precision in alignment at bare-die level. Precise details of the entire integration flow and the materials are provided in the methods section.

2.3. Material Optimisations for Marine Environment

Marine species experience varying oceanic environments during their natural movements, migration, and foraging for food and evading predation. An electronic tagging system must be able to withstand these varying extreme conditions an individual experiences.

The temperature of seawater drops from 27 °C at the surface to 2 °C as the depth reaches approximately 4000 m, highlighting the need for highly sensitive temperature sensors for detection of small variations. [4,42] Traditionally, gold has been a primary material choice for biological applications due to desirable properties like biocompatibility, corrosion resistance, and non-toxicity. Consequently, in our Marine Skin version 1, we used Au as the metal for all the sensors and interconnects. However, Platinum is widely known for its usage in RTD sensors therefore, we compared our version 1 and version 2 of Marine Skin having Au and Pt as a temperature sensor. **Figure S1** represents drastic improvement (10 folds) in the temperature sensitivity from 43.18 mΩ/°C for Au in version 1 to 487.5 mΩ/°C for Pt in version 2.

In our previous work, we reported the reliable performances of the sensory platform in the controlled environment with a maximum depth of 1 m. For any pressure higher than 1 m depth, the sensor's response to pressure diminished in version 1 and saturated at the moderate pressure of 10 m. We observed that the device retained its performance when recovered from the water after subjecting it to the higher depth. We chose PDMS due to its compressive nature as a dielectric material for capacitive pressure monitoring underwater. We observed increased sensitivity, and the increased range for depth detection for an optimized thickness of 50 μm dielectric PDMS layer

with 1:12 ratio of curing agent to elastomer **(Figure S3)** (see supplementary information for details).

Although the optimization in dielectric thickness and the composition resulted in improved sensitivity, we observed the saturation in pressure detection at depths higher than 10 m. We hypothesized that this saturation is due to mechanical stress distribution on the thin metallic layer. The metal layers (Au in version 1 or Cu in version 2) are sandwiched between the very compliant materials such as PDMS and PI (**Figure 3a**), so we can postulate that metal/polymer interface might experience the maximum stresses. Thus, finite element methods (FEM) model was created using COMSOL Multiphysics to understand the mechanical stress distribution due to high pressure at the interface of sandwiched metal in the polymer. **Figure 3b** illustrates the linear increase in the stresses at the metal interface for both thin Au/Ti (150 nm/10 nm) and thick Cu (5 µm) metal. It is evident that stresses are higher for Au whereas corresponding values for Cu are lower. As expected, the thick layer of Cu has lower stresses (σ_{max} = 1.5 GPa) compared to Au (σ_{max} = 5.8 GPa). The stress contours for the small region with Au is shown in **Figure 3c**. The thickness of Au/Ti in version 1 deposited on the PI substrate could not sustain the stresses exerted on the metal/PI interface and hence creates a discontinuity in the film to give a saturated response with external pressure. As the elastic modulus of Au is slightly lower than that of Cu, Au is expected to induce lower stresses when using the same thickness for both materials (i.e. Cu and Au). However, it is clear from the simulations that the difference of induced stresses for both materials is insignificant, which does provide a sound reason to adopt the inexpensive Cu material for the device. It is evident that evolved stresses depend on the elastic modulus and feature size, thus the thicker metal would result in the lower stresses. It is further proved by simulations that a relatively thick metal (~5 µm compared to 150 nm) reduces the stresses significantly. **Figure 3d** shows that

stress has reduced significantly, which reveals the benefit of using a relatively thicker layer of Cu. And when a thick metal (sub 10 µm) is to be selected, it only makes sense to elect a material that is significantly cheaper and can be readily grown/deposited using a simple technique. Thus, we chose Cu over expensive Au which can be easily deposited using ECD technique. Conducted experimental results of sustained performance at higher pressure validate the FEM results.

2.4. Sensory System Performance

This version 2 of the Marine Skin is advancing the previous version 1 in terms of its performance in harsh marine environmental conditions. Since the temperature of seawater drops from 24 °C at the surface to 2 °C at ~4000 m depth, it is important to capture the small variations throughout which means a sensor with high sensitivity. From **Figure 4b**, reliable linearity of the temperature sensor is evident from by the correlation of $R^2 = 0.99872$. Moreover, the calculated sensitivity of version 2 ($S_{v2} = 358.8$ mΩ/°C) is ~15 times higher than the version 1 ($S_{v1} = 22.66$ mΩ/°C). In addition, version 1 had a large variation in performance when immersed in water compared to in air performance, more pronounced in the range of interest of temperature change (0-21 °C, the range of interest for sea environment). In version 2, we not only observe sustained linearity (constant sensitivity) over the entire regime from ~2 °C to 60 °C but also the performance of matches with the existing commercial solution for the temperature sensor **(Figure S1b)**. Thus, making it more reliable and a feasible alternative for direct integration with the SoC device.

The electrical conductivity of the aqueous solution is the measure of salinity. Version 1 of the salinity sensor design was a simple two electrodes design (2 mm apart) which conducts an electrical current when an ionic solution bridges the electrodes. Version 1 salinity sensor demonstrated reasonable performance with an average sensitivity of 3.298 kΩ/PSU. To increase

the reliability and sensitivity further, we adopted an interdigitated electrode pattern. This modified design resulted in tremendous increased average sensitivity to a value of 19.655 kΩ/PSU (recording ~500% increase). We have observed a change of ± 3% in the baseline values when submerged in seawater for extended periods (28 days), however, the sensitivity of the device has not changed significantly as shown by the hysteresis plot in **Figure 4c**.

In version 1, the pressure sensor has shown a very stable response to changes in the water pressure due to increasing depths (shown by 5 cm steps), however, the response saturated when the height of water goes > 10 m. Although, many marine species swim in depths < 600 m, there are also many deep-sea species that inhabit depths around 3000 m (Vampire squid) and 4500 m (Pacific Viperfish). Thus, we have optimized the material for sustaining the performance up to 2000 m. **Figure 4d** illustrates the linear response to a linear increase in depth in steps of 30 m each. We have not observed any saturation in the pressure sensor response even up to 2000 m, which is the ultimate limit of the compression tank. Thus, we infer that version 2 with optimized design and the material shows sustained performance in harsh environments with all the enhanced performance metrics compared in **Table 1.** Such high-pressure sustainability and the capability has never been reported previously.

2.5. *Rugged Performance*

The reliability of encapsulation material can be established if the Marine Skin platform shows no degradation in performance under rugged and harsh environmental testing conditions. It must not be affected by any external factors. Since we have no control over the orientation of the animal movement or their rotation, it is important to have a device that has no dependency on the orientation of the sensor (or the orientation/rotation of the animal). We carried out depth measurements in two different orientation (horizontal and vertical) to correlate if there is any

dependency. The rationale for choosing pressure sensor lies in its working principle of capacitive sensing, as the capacitive sensor can experience different pressures in different orientations at the same height inside water. **Figures 5a** and **5b** plot the hysteresis curves for the depth measurements in the horizontal and vertical orientation of the sensor. There was no significant change observed due to the orientation of the sensor, in addition, the hysteresis curves represent the consistency of the results.

The benchmark for testing the reliability and robustness of any flexible device is the sustained performance over multiple physical deformations (bending cycles). Here, we establish a record benchmark for the robustness and ruggedness of the soft-polymeric packaging and sensor design by subjecting sensors under the extreme number of bending cycles. We subject the Marine Skin version 2 to cyclic bending testing for 10 thousand cycles, with each cycle bending the sensor with a radius of 1 mm and stretching **(Figure 5f)** (**Supplementary Video S1**). The device is characterized at the intervals of 0, 100, 500, 1000, 2500, and 10000 cycles respectively. From **Figure 5c**, we observe that median temperature sensitivity stands at 330.45 mΩ/°C with minute variations in absolute sensitivities at specific cycles. However, the change in sensitivity recorded is < 4% from the value at zero bending cycles. Similarly, the robustness of the pressure sensor can be observed from **Figure 5d** where the sensitivity has not changed significantly due to constant cyclic physical deformations. The observed variations are mainly due to manual controlling of the immersion in water, whereas the maximum deviation observed in absolute value is < 2.6% from the initial baseline at zero cycles.

Similarly, the effect of prolonged exposure to the Red Sea saline water (41 PSU) is studied for establishing robustness and reliability of the packaging. The packaged sensors were immersed in the Red Sea water for extended periods of time while their performance is evaluated after 1, 3, 7,

15, and 28 days. Once again, there is no significant noticeable variation in performance observed for pressure sensors as illustrated in **Figure 5e**. Moreover, the maximum deviation in an absolute value of recorded pressure is < 2.3% from the average value at maximum depth. It must be noted that the cyclic testing was carried out on the samples, which were already exposed to Red Sea water for ~ 1 month, and hence it establishes more robust packaging by showing reliability.

For deployment on the animals and monitoring the required parameters, the utmost important aspect is the sustained performance at high depths, which no other research has reported. In **Figure 4d**, we can clearly observe the linear increment in the capacitance as the pressure increases and retaining the similar step change over the entire range from 500 m to 1500 m. The real-time oscillations due to fluctuations in the pressure are plotted in **Figure S4**, suggesting high resolution and excellent sensitivity. This linear variation in the depth measurement along with no saturation even at the depth of 2000 m (limited due to the experimental emulator equipment's range) suggest robust and sustained performance at extreme environments. This is the first instance where we report the sustained performance of the devices at such high depth which has never been reported by any other groups previously.

To summarise, the modified design and material optimization of Marine Skin version 1 has resulted in a tremendous increase in sensitivity, reliability, and robustness of the packaging. In addition, version 2 demonstrates extremely robust and rugged performance reported for the first time, in an extremely harsh environment 10^4 bending cycles (bending radius 1 mm), high pressure (3000 psi, ~2 km), and prolonged immersion in Red Sea water (1 month at 41 PSU).

2.6. Attachment Strategies for Deployment

Marine species have huge variations in their skin types. Many fish species have skeletal elements (scales) that cover their skin. Scales are classified based on the composition and structure

as Ganoid scales, Placoid scales (or denticles), Cycloid scales, and Ctenoid scales. [43] Careful consideration must be given to the skin type of the species under study for devising the best attachment method. Sharks are one of the most widely studied and tagged marine species for several reasons. For instance, the Silky shark (*Carcharhinus falciformis*) is one of the most abundant cosmopolitan shark species of the pelagic zone. It feeds on schooling fishes, including tuna, and as a result is a major bycatch item of the tuna fishery. Typically, shark skin is very rough with huge denticles scattered over the skin each with the pulp cavity surrounded at the edge with odontoblasts. In addition, the animals often used for tagging of bio-loggers include hard shell bodied crustaceans and sea turtles. [29,43,44] Most of the work on tagging constitutes mainly invasive attachment methods with attachment methods using incisions and anchors. Our initial tagging experiment with version 1 relied on a host body (like a cylindrical CAN platform) (**Supplementary video S2**) for non-hard shell animals, which are attached to the dorsal fin of the sharks using clamps (3D printed and/or metallic) as shown in the **Figure 6a**. These clamps not only exert pressure on the fins of sharks but also attract other individuals to attack this foreign element. Moreover, this methodology does not comply with the smaller fishes and the species that do not have rigid fins.

We have tagged a wobbegong shark and stingray with a very different skin type using dental glue (**Figures 6c** and **6d**). The tag stayed perfectly conformal to the body of the animal (**Supplementary Video S3**), however, surgical glue dissolves in water within 48 hours and prolonged deployment was not possible. We observed that any tagging platform, which is not conformal to the skin will detach in a short time due to the hydrodynamic forces acting on the tags in the opposite of the swimming direction. It has been noticed from veterinary experts' that permanent glue and/or super adhesives present the danger of skin irritation and injuries to the soft

skin of the species. For small and bony fishes, the skin is very soft and has mucous membranes. Furthermore, there are species such as dolphins that are known to replace their skin cells over short time periods (< 1 day). Hence, alternative strategies for attachment needs exploration.

Consequently, we present a unique, pragmatic, and universal approach for sensory platform tagging. We propose a soft wearable bracelet in which the sensory tags can be embedded (**Figure 6f (**right)) within the soft polymer (PDMS) that can be wrapped around species like a wearable gadget. Flexibility, direct compatibility with the schematic flow, biocompatibility, softness, elasticity, and other properties of PDMS played an important role in material choice. The interlocking mechanism of the jacket consists of 3D printed mushroom pins that lock into holes on the other side of the bracelet (**Figure 6g** (right)). The presence of multiple pins allows adaptability of the same gadget for different sized animals. The strength of the bracelet was tested in the lab by wrapping it around closed fingers and stretching to see if the interlocking parts break (**Figure S9e**) and the device did not break even after exerting significant force. We illustrated the attachment mechanism by tagging the Barramundi *(Lates calcarifer)* and Seabream (**Figure 6f and 6g**). We have observed, that this wearable Marine Skin is easy to attach even on small fishes. It presented no hindrances to their natural movements due to softness, conformability, stretchability, and minimal weight (bracelet with the embedded system weighs < 3g) (**Supplementary Video S4 and S5**). Hence, the feather-light and breathable wearable bracelet pattern is a pragmatic mechanism for the Marine Skin tagging system that is conformal, comfortable for not only the individual species tagged but also not noticeable for the other species due to its inherent transparency.

3. CONCLUSION

The ocean ecosystem is affected by multiple human impacts like pollution, over-exploitation, warming, and acidification. To facilitate the policy implementations, trade-offs and devise mitigation strategies at global scales, it is very important to quantify the distribution of the human impacts on the marine environment and hence marine research should include ocean wide monitoring of species and the environment. Monitoring should also include the deep ocean which covers a majority of the earth's surface but remains poorly studied. The evolution of the sensors and tracking tools in conjunction with the advances in the technology is making pivotal contributions in understanding the marine ecosystem and animal behavior and it will continue to grow further. The complex animal geometries, different skin types, size, and varying environmental conditions necessitate a flexible wearable and stretchable gadget that can monitor different environmental parameters without any discomfort to the animal. Recently, we have demonstrated a flexible, and stretchable waterproof Marine Skin platform for monitoring the environment, however, for the harsh environment and the varying conditions, a rugged and robust device is required. Therefore, we demonstrate an extremely rugged and robust version of the Marine Skin tagging platform that withstood 10^4 severe bending cycles (1 mm bending radius), prolonged exposure to the highly saline (41 PSU) Red Sea water, and the extremely high pressure of ocean depths (~ 2 km deep). To facilitate ocean monitoring, a unique attachment strategy by means of a wearable stretchable jacket (gadget) architecture is implemented for a non-invasive and easy attachment method without any harm and discomfort to the species irrespective of their skin type. This Marine Skin gadget outperforms any other entities in the domain in terms of flexibility, stretchability, non-invasiveness, comfort, featherlight (weight <0.5g for systems, and <3 g with the entire wearable gadget), with proven ruggedness and sustained performance at high pressure.

4. METHODS

4.1. *Fabrication of the sensors*

We start with two Si (100) wafers and spin 10 μm polyimide (PI 2611 from HD Microsystems) at the speed of 2000 rpm for 30 seconds. PI needs multiple curing steps of soft-baking, intermediate and final curing at different temperatures. Soft-baking is performed for 90 s at 90 °C, intermediate baking at 150 °C for 90 s and final curing at 300 °C for 30 minutes while the temperature should be gradually ramped at the rate of 240 °C /hr to reach 300 °C from 150 °C. The step of PI spinning and later releasing the PI is depicted in **Figure 2d**. In parallel, we use another wafer as the carrier for the encapsulation from the bottom side using PDMS. We take a 300 nm silicon oxide deposited on Si (100) wafer followed by sputtering a thin layer (10 nm/100 nm) of Ti/Au. This gold film is used due to its low bonding energy with PDMS and hence it eases the process of peeling the entire sensory platform when final encapsulation is completed. 100 μm of PDMS is spun in at 500 rpm speed for 60 s followed by curing at a relatively low temperature of 70 °C for 45 minutes. PDMS for encapsulation layers (bottom and top) is prepared by mixing elastomer to curing agent (Sylgard 184^{TM}) in the ratio of 10:1.

We perform O_2 plasma treatment of PI on wafer 1 followed by deposition of 100 nm Cu using sputtering. O_2 treatment of PI helps in having better adhesion of the deposited metal. Cu is used as a seed layer for deposition of a thick (10 μm) Cu by using ECD technique. The growth of ECD Cu is restricted to only the desired pressure sensor pattern by using a lithography. The growth of the first metal layer ECD Cu is followed by PR removal and removal of Cu seed layer using plasma etching. The temperature sensor was fabricated in the next step by a lift-off process and sputtering a 100 nm of Pt. The plasma etching of PI follows Cu seed removal to pattern the PI for introducing the stretchability by design geometry. Compressive soft dielectric material PDMS (50 μm at 700

rpm for 60s) is then spun on the patterned bottom metal layer. After dielectric PDMS is cured, we transfer the second layer of PI on this layer and repeat the steps for top layer ECD Cu.

Once the seed layer is removed and PI is etched for the top metallic layer, the entire stack is transferred onto wafer 2, which has 100 μm PDMS cured on it. A transfer is followed by integration of SoC and battery using a modular LEGO electronics approach with the help of pick-and-place robotic tool customized to handle the flexible substrates and ICs. [23] The placement accuracy is as high as ±3 μm with ~7000 UPM (units per module) production rate, which shows the manufacturability of the process. Finally, the entire systems integrated is encapsulated for waterproofing using 100 μm PDMS (1:10 ratio of curing agent: elastomer). Salinity sensor pattern is on the top metal seed layer and it has to be directly exposed to the aqueous solution, which was achieved by laser cutting the PDMS around the active area of the salinity sensor, thereby not compromising any other packaging.

4.2. Saline Solution Preparations

The salinity of seawater is mainly the concentration of ions predominantly NaCl, in addition to a lower percentage of Magnesium, Calcium, Strontium, and Potassium. Thus, the conductivity of the saline water changes with the concentration of these ions. The salinity of the seawater mainly ranges from 30 PSU to 40 PSU [27], [34]. 1 PSU corresponds to 1 part per thousand (ppt) of the NaCl in 1 kilogram of water. 1 PSU = 1 ppt = 1 g of salt/kg of water. For this work, the salinity solutions were prepared accordingly from salinity range between 5 to 45 PSU by adding 5-45 mg of NaCl in the deionized (DI) water. Measurements for the salinity sensors are done by making a small cavity of PDMS surrounding the active sensing area by which the probing electrodes will not be in direct contact with the saline solution. A drop of saline solution is held in the active area and the resistance was measured followed by removal of the solution using a blower. This method of

having a cavity and blowing away the solution provided more stable and consistent measurements compared to other conventional methods of dipping the entire sensor in the solution.

4.3. Temperature measurements

The variation in the oceanic temperature mainly falls in the range of 2 °C - 27 °C depending on the location and depth of the water. In the lab environment, we tested the temperature sensor from ~5 °C up to 85 °C. A temperature of 5 °C was maintained by putting the sample on an ice bath, however, we did not have the control on the ramping of temperature up to room temperature. We used a programmable hot plate to control the temperature above room temperature in steps of 5 °C, though some variations were observed in the exact temperature and the set temperatures.

4.4. High Depth Sensor Measurements

For material optimization and the robustness testing, measurements were carried out in an acrylic tank of height 1 m filled with Red Sea water in the lab. For high-pressure measurements, we used a compression chamber, which can simulate and control the pressure related to the depth manually or digitally up to a depth of 2000 m. A metallic cylindrical chamber of 60 cm height (15 cm diameter) filled with Red Sea water and the sensor is placed inside the chamber connected with the waterproof connectors for connecting the Keithley **(Figure S4)**. Manual pressure was applied using hydraulic weights and piston in steps of 30 m height (43 psi) until it reaches the pressure equivalent to a height of 1500 m. Manual pressure application was preferred over digital due to the interference of the electrical signal on the measurements in addition to being enclosed in a metallic cylinder. A maximum of 3000 psi pressure could be applied using this chamber until which we could see no saturation in the measurements, however, the pressure was not stable above 2300 psi due to the limitation of the tool. Thus, the measurements were restricted to 1500 m (2200 psi) depth.

4.5. Animal tagging

For devising the efficient tagging and attaching mechanism for the developed compliant sensors, it was important to conduct the trials live on the field with the species that are not hard-shell bound. We carried out the initial attachment methods using different surgical dental glues, 3D printed and steel clamps, suction cups on a wobbegong shark, stingray, tiger shark, and dolphin at the Oceanografic Marine facilities in Valencia, Spain. The basic understanding and the challenges from the experience of this field-testing helped in devising a better attachment mechanism using a wearable gadget that was tested on barramundi, common goldfish, and sea bream in the KAUST core lab facilities. Tests were conducted following IUCUC guidelines (approved IACUCML application number #18-01-015 at KAUST).

4.6. Numerical modeling

We used numerical analysis technique to compare the performances of Au and Cu in the full stack of the marine sensor, under same pressure conditions i.e. forces experienced by the structure under the water depth of 1000 m. The geometrical parameters were taken identical to the experiments. We used a linear elastic Solid Mechanics module of a commercial FEM program COMSOL™ to map the structural response i.e. mechanical stress distribution. Since no permanent bending or deformation was observed in our device, it is reasonable to use the linear elastic mechanics in the modeling to simplify the calculations. Furthermore, it is well established that for a linear elastic mechanics, the stresses are linearly proportional to the strains which are expected to exceed the yield strength of the materials under large loading when plasticity is not considered in the model. This holds true for our model where we have assumed it to be an elastic model based on experimental observation of no plastic deformations in the devices. The bottom surface of the PDMS was kept as a fixed boundary while symmetric conditions on the sides of the stack were

applied. To exert the equivalent forces of water at the corresponding depth, sweep function of boundary load (equivalent pressure) on top surface was implemented. Elastic moduli of Au, Cu, PDMS, and Pi were takes as 70 GPa, 120 GPa, 2.9 MPa, and 8.5 GPa, whereas the Poisson's ratio as 0.44, 0.34, 0.49, and 0.40, respectively. To make sure that the solution is converged, a fine mesh was considered.

5. ACKNOWLEDGMENT

This publication is based upon work supported by the King Abdullah University of Science and Technology (KAUST) Office of Sponsored Research (OSR) under Award No. Sensor Innovation Initiative OSR-2015-Sensors-2707 and KAUST-KFUPM Special Initiative OSR-2016-KKI-2880. We thankfully acknowledge Oceanografic Valencia, Spain for helping with the marine species based testing of the reported "marine skins", and Jorge Alarcon and the Beacon Corporation for assistance with fish husbandry at KAUST. We declare no competing financial interest.

REFERENCES

[1] J. B. C. Jackson, M. X. Kirby, W. H. Berger, K. A. Bjorndal, L. W. Botsford, B. J. Bourque, R. H. Bradbury, R. Cooke, J. Erlandson, J. A. Estes, T. P. Hughes, S. Kidwell, C. B. Lange, H. S. Lenihan, J. M. Pandolfi, C. H. Peterson, R. S. Steneck, M. J. Tegner, R. R. Warner, *Science (80-.).* **2001**, *293*, 629.

[2] B. S. Halpern, S. Walbridge, K. A. Selkoe, C. V. Kappel, F. Micheli, C. D'Agrosa, J. F. Bruno, K. S. Casey, C. Ebert, H. E. Fox, R. Fujita, D. Heinemann, H. S. Lenihan, E. M. P. Madin, M. T. Perry, E. R. Selig, M. Spalding, R. Steneck, R. Watson, *Science (80-.).* **2008**, *319*.

[3] C. M. Duarte, *Front. Mar. Sci.* **2014**, *1*, 63.

[4] USEPA, "Climate Change Indicators: Stream Temperature," can be found under https://www.epa.gov/climate-indicators/climate-change-indicators-sea-surface-temperature, **2016**.

[5] in *Int. Geophys.*, **1994**, pp. 171–203.

[6] J. M. Nassar, S. M. Khan, S. J. Velling, A. Diaz-Gaxiola, S. F. Shaikh, N. R. Geraldi, G. A. Torres Sevilla, C. M. Duarte, M. M. Hussain, *npj Flex. Electron.* **2018**, *2*, 13.

[7] H. A. Broadbent, T. P. Ketterl, C. S. Reid, J. Dlutowski, in *Ocean. 2010 MTS/IEEE SEATTLE*, IEEE, **2010**, pp. 1–7.

[8] C. J. Bridger, R. K. Booth, *Rev. Fish. Sci.* **2003**, *11*, 13.

[9] N. Jepsen, C. Schreck, S. Clements, E. B. Thorstad, *Aquat. Telem. Adv. Appl. Proc. Fifth Conf. Fish Telem.* **2003**, 255.

[10] C. C. Wilmers, B. Nickel, C. M. Bryce, J. A. Smith, R. E. Wheat, V. Yovovich, *Ecology* **2015**, *96*, 1741.

[11] R. S. Brown, S. J. Cooke, W. G. Anderson, A. R. S. Mckinley, *North Am. J. Fish. Manag.* **1999**, *19*, 867.

[12] S. J. Cooke, S. G. Hinch, M. Wikelski, R. D. Andrews, L. J. Kuchel, T. G. Wolcott, P. J. Butler, *Trends Ecol. Evol.* **2004**, *19*, 334.

[13] K. A. Walker, A. W. Trites, M. Haulena, D. M. Weary, *Wildl. Res.* **2012**, *39*, 15.

[14] S. Andrzejaczek, A. C. Gleiss, L. K. B. Jordan, C. B. Pattiaratchi, L. A. Howey, E. J. Brooks, M. G. Meekan, *Sci. Rep.* **2018**, *8*, 8351.

[15] L. A. Howey-Jordan, E. J. Brooks, D. L. Abercrombie, L. K. B. Jordan, A. Brooks, S. Williams, E. Gospodarczyk, D. D. Chapman, *PLoS One* **2013**, *8*, e56588.

[16] A. C. Broderick, B. J. Godley, *Anim. Behav.* **1999**, *58*, 587.

[17] K. Alex Shorter, M. M. Murray, M. Johnson, M. Moore, L. E. Howle, *Mar. Mammal Sci.* **2014**, *30*, 726.

[18] N. Hammerschlag, S. J. Cooke, A. J. Gallagher, B. J. Godley, *Methods Ecol. Evol.* **2014**, *5*, 1147.

[19] T. Todd Jones, K. S. Van Houtan, B. L. Bostrom, P. Ostafichuk, J. Mikkelsen, E. Tezcan, M. Carey, B. Imlach, J. A. Seminoff, *Methods Ecol. Evol.* **2013**, *4*, 1178.

[20] A. M. Hussain, M. M. Hussain, *Adv. Mater.* **2016**, *28*, 4219.

[21] S. F. Shaikh, M. T. Ghoneim, G. A. Torres Sevilla, J. M. Nassar, A. M. Hussain, M. M. Hussain, *IEEE Trans. Electron Devices* **2017**, *64*, 1894.

[22] J. M. Nassar, J. P. Rojas, A. M. Hussain, M. M. Hussain, *Extrem. Mech. Lett.* **2016**, *9*, 245.

[23] S. F. Shaikh, M. T. Ghoneim, R. R. Bahabry, S. M. Khan, M. M. Hussain, *Adv. Mater. Technol.* **2018**, *3*, 1700147.

[24] N. E. Hussey, S. T. Kessel, K. Aarestrup, S. J. Cooke, P. D. Cowley, A. T. Fisk, R. G. Harcourt, K. N. Holland, S. J. Iverson, J. F. Kocik, J. E. Mills Flemming, F. G. Whoriskey, *Science (80-.).* **2015**, *348*.

[25] F. Tonolini, F. Adib, **n.d.**, DOI 10.1145/3230543.3230580.

[26] C. Shen, Y. Guo, H. M. Oubei, T. K. Ng, G. Liu, K.-H. Park, K.-T. Ho, M.-S. Alouini, B. S. Ooi, *Opt. Express* **2016**, *24*, 25502.

[27] A. Al-Halafi, H. M. Oubei, B. S. Ooi, B. Shihada, *J. Opt. Commun. Netw.* **2017**, *9*, 826.

[28] H. M. Oubei, C. Shen, A. Kammoun, E. Zedini, K.-H. Park, X. Sun, G. Liu, C. H. Kang, T. K. Ng, M.-S. Alouini, B. S. Ooi, *Jpn. J. Appl. Phys.* **2018**, *57*, 08PA06.

[29] R. E. Hueter, J. P. Tyminski, F. Pina-Amargós, J. J. Morris, A. R. Abierno, J. A. A. Valdés, N. L. Fernández, *Bull. Mar. Sci.* **2018**, *94*, 345.

[30] W. Gladstone, C. R. Facey, K. Hariri, **1996**.

[31] L. S. Balistrieri, J. W. Murray, *Geochim. Cosmochim. Acta* **1987**, *51*, 1151.

[32] H. Zhang, M. Chiao, *J. Med. Biol. Eng.* **2015**, *35*, 143.

[33] M. Huang, H. Yan, C. Chen, D. Song, T. F. Heinz, J. Hone, *Proc. Natl. Acad. Sci. U. S. A.* **2009**, *106*, 7304.

[34] S. Krishnan, C. J. Weinman, C. K. Ober, *J. Mater. Chem.* **2008**, *18*, 3405.

[35] M. J. Vucko, A. J. Poole, C. Carl, B. A. Sexton, F. L. Glenn, S. Whalan, R. De Nys, A. J. Poole, C. Carl, B. A. Sexton, F. L. Glenn, S. Whalan, **2014**, *7014*, DOI 10.1080/08927014.2013.836507.

[36] C. Liu, C. Ma, Q. Xie, G. Zhang, **2017**, 15855.

[37] N. Qaiser, S. M. Khan, M. Nour, M. U. Rehman, J. P. Rojas, M. M. Hussain, *Appl. Phys. Lett.* **2017**, *111*, 214102.

[38] J. E. Mark, *J. Am. Chem. Soc.* **1999**, *131*, 1012.

[39] A. Furniturewalla, M. Chan, J. Sui, K. Ahuja, M. Javanmard, *Microsystems Nanoeng.* **2018**, *4*, 20.

[40] Z. Huang, Y. Hao, Y. Li, H. Hu, C. Wang, A. Nomoto, T. Pan, Y. Gu, Y. Chen, T. Zhang, W. Li, Y. Lei, N. Kim, C. Wang, L. Zhang, J. W. Ward, A. Maralani, X. Li, M. F. Durstock, A. Pisano, Y. Lin, S. Xu, *Nat. Electron.* **2018**, *1*, 473.

[41] J. Viventi, D. H. Kim, L. Vigeland, E. S. Frechette, J. A. Blanco, Y. S. Kim, A. E. Avrin, V. R. Tiruvadi, S. W. Hwang, A. C. Vanleer, D. F. Wulsin, K. Davis, C. E. Gelber, L. Palmer, J. Van Der Spiegel, J. Wu, J. Xiao, Y. Huang, D. Contreras, J. A. Rogers, B. Litt, *Nat. Neurosci.* **2011**, *14*, 1599.

[42] S. C. Doney, M. Ruckelshaus, J. Emmett Duffy, J. P. Barry, F. Chan, C. A. English, H. M. Galindo, J. M. Grebmeier, A. B. Hollowed, N. Knowlton, J. Polovina, N. N. Rabalais, W. J. Sydeman, L. D. Talley, *Ann. Rev. Mar. Sci.* **2012**, *4*, 11.

[43] "Integument - Fishes | Britannica.com," can be found under https://www.britannica.com/science/integument/Fishes, **n.d.**

[44] R. Bonfil, *Sharks Open Ocean Biol. Fish. Conserv.* **2009**, 114.

TABLES

Table 1: Comparison of the performance matrices for two versions of Marine Skin.

Parameter	Previous	Present	% change
Average temperature sensitivity	22.66 mΩ/°C	***358.8 mΩ/°C***	***~1500 %*** increase; (***14.83 folds*** increase)
Average salinity sensitivity	3.298 kΩ/PSU	***19.655 kΩ/PSU***	***~500 %*** increase
Maximum depth of sustenance	< 10 m	~ ***2000 m***	***200*** fold increase
Weight	~ 6 g	< ***3 g*** entire gadget; < ***0.5 g*** (sensor with dies, without bracelet)	*50%* decrease even after addition of wearable bracelet
Bending cycles	N/A	**> 1 × 10^4**	N/A
Saline water prolonged exposure	20 days	28 days	Both versions can withstand

*Note: Comparison with other commercial products have already been presented in the previous work,[6] which stands true for this version as well.

FIGURES

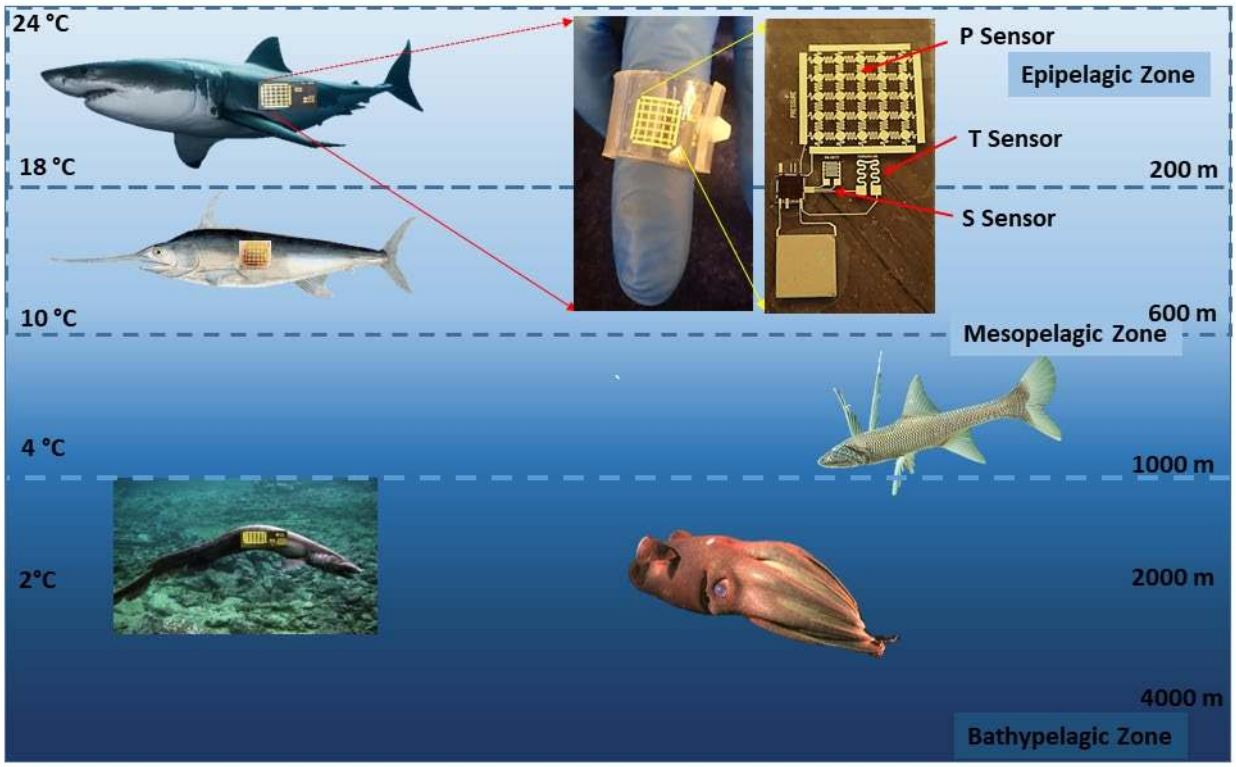

Figure 1: Robust compliant Marine Skin illustration. Different marine species swimming at varying depths under the dark see and respective temperature ranges experienced. The digital photograph of the multisensory wearable Marine Skin tagging gadget for marine environmental monitoring.

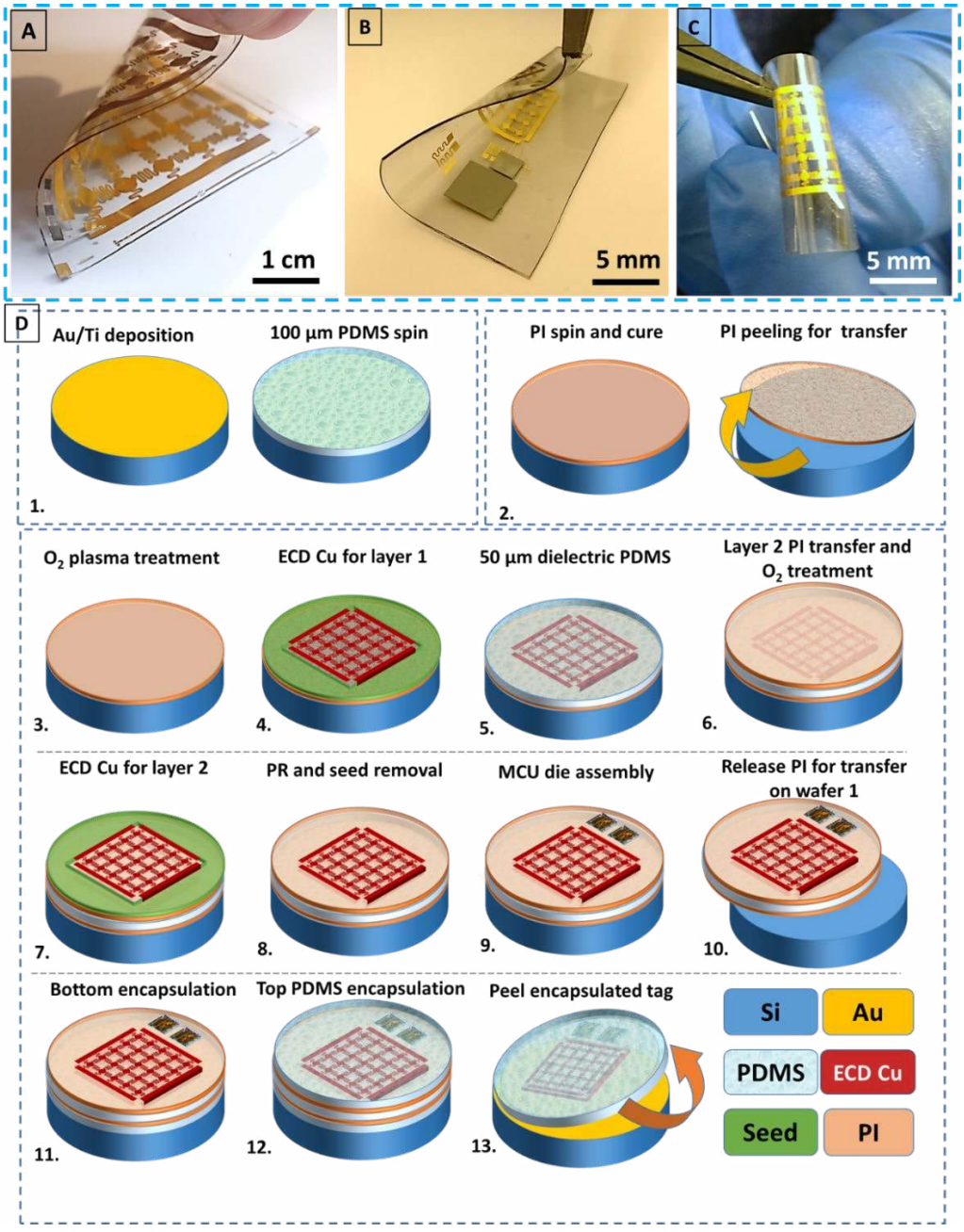

Figure 2: 3D schematic process integration for the waterproof and featherlight Marine Skin platform, (**A-C**) represents version 1 (modified with bare die ICs), version 2 and the extreme bending of the tag respectively. (**D**) Steps involved in the process, Wafer 1 for the bottom PDMS encapsulation spun on Ti/Au for ease of removal is shown in **stage 1**. S**tage 2** shows polyimide (PI 2611) spun and peeled for transfer at later stages. **Steps 3-8** represents fabrication of sensors layers and patterning using different processes. **Step 9** presents the die integration of microcontroller and battery dies for a stand-alone system using a pick-and-place tool. **Step 10-13** illustrates transfer for a bottom and top waterproof encapsulation of the entire system with the final release from the wafer. Bottom inset shows the final released lightweight, extremely compliant Marine Skin platform.

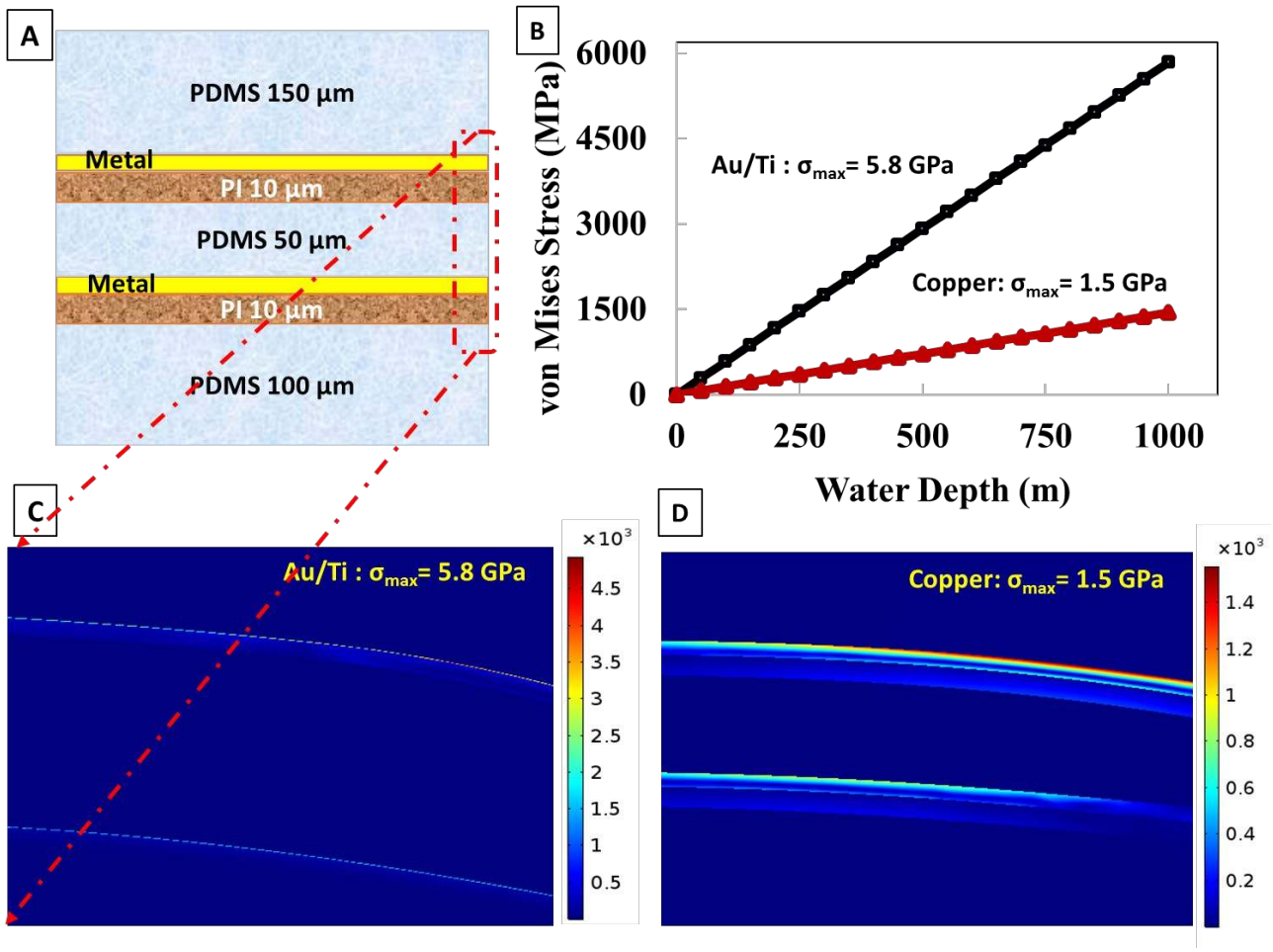

Figure 3: FEM simulation studies to understand the stress distribution at the metal/polymer interface. **(A)** Cross section profile of the sensory platform showing different layers (not to scale). Yellow layer represents metal. **(B)** von Mises stress experienced by the metallic interface at different depths under water, Cu experiencing significantly lower experiences than Au/Ti. **(C)** and **(D)** stress distribution contours at the sandwiched interface of polymers and metals.

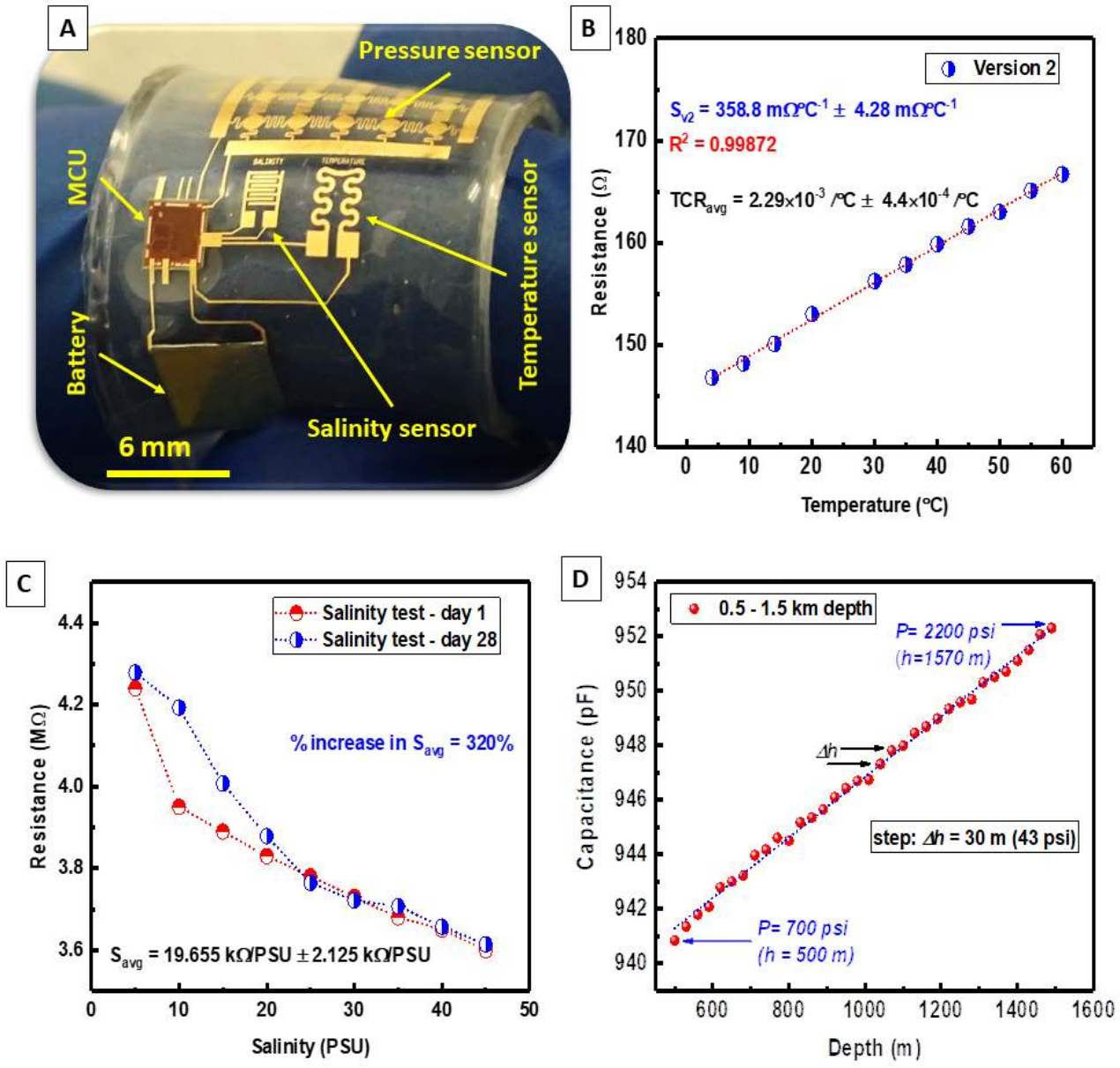

Figure 4: Performance improvement of the wearable multisensory Marine Skin gadget with a reliable interlocking mechanism showing all the components in **(A)**. Improved sensing capabilities from version 1 for sustaining higher pressure and improved **(B)** temperature sensitivity, with great linearity and **(C)** salinity sensor with increased sensitivity and reliable hysteresis for prolonged saline water exposure. **(D)** Depth measurements for higher depths (high pressure) 1.5 km, increments in the steps of 30 m each, representing the linear fit throughout the entire range.

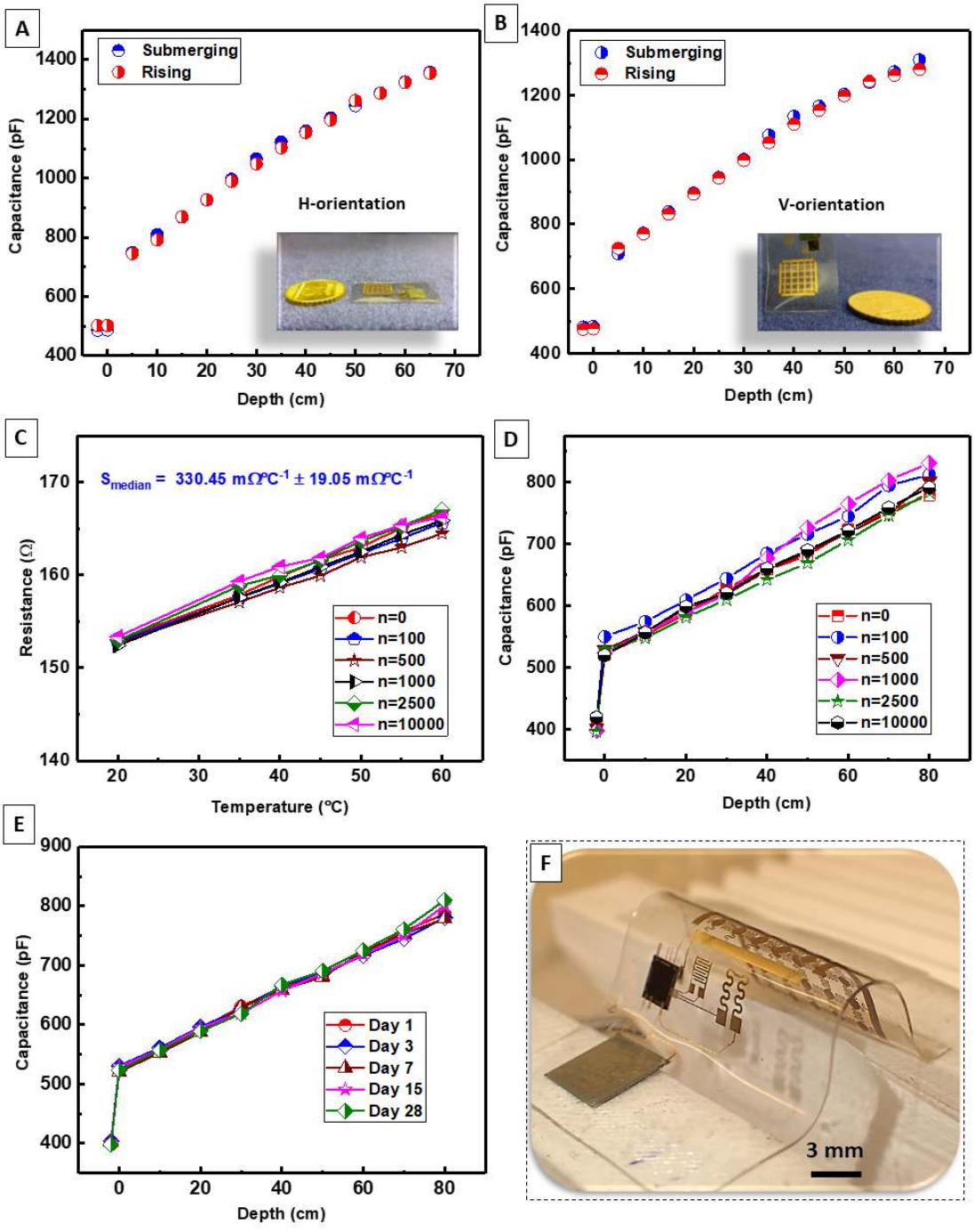

Figure 5: Robustness and reliability of the devices for prolonged exposure to highly saline seawater and the cyclic bending testing. Reliable depth sensing performance and hysteresis (submerging in water and raising from water) independent of the sensor orientation **(A)** horizontal or **(B)** vertical orientation with respect to the ground plane. Harsh bending cycle testing for **(C)** temperature sensors and **(D)** depth sensor, by subjecting to a bending radius of 1 mm for a maximum 10^4 cycles. **(E)** Effect of prolonged exposure to highly saline Red Seawater on depth sensing for 1, 3, 7, 15, and 28 days. **(F)** Bending cycles test setup for cyclic testing, Version 2 Skin in stretched and then bent for a bending radius of 1 mm.

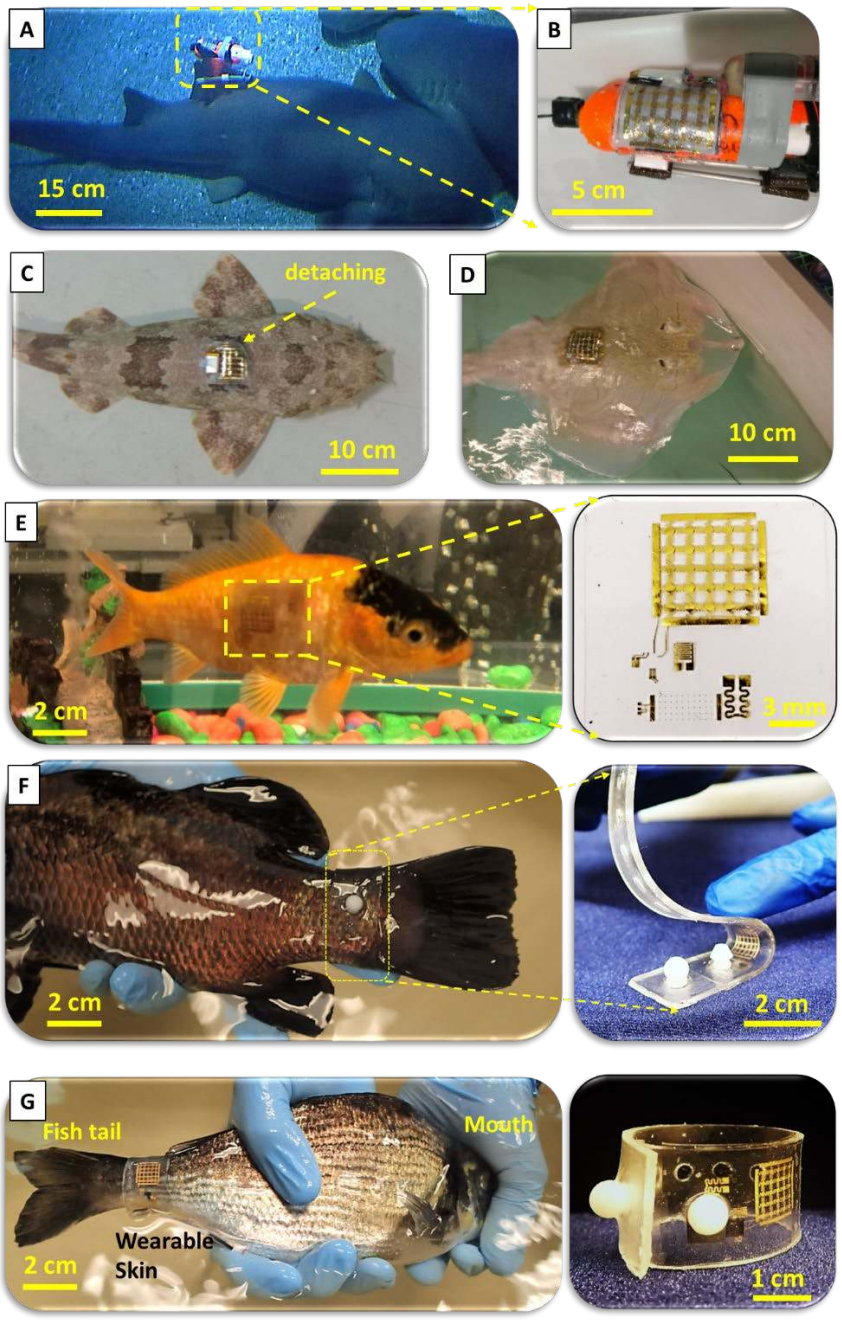

Figure 6: a Non-invasive attachment mechanism for tagging Marine Skin. **(A)** Shark tagged using a steel clamp attached to a light cylindrical can **(B)** hosting the Marine Skin platform. Direct tagging version 1 using surgical glue on **(C)** wobbegong shark, **(D)** Stingray popping out due to the water stream and the rigid component of the battery. **(E)** Scaled version 2 without rigid components adhere strongly on goldfish attached using surgical glue. **(F)** Direct tagging of Marine Skin version 2 on the barramundi fish (left) using wearable soft bracelet with sensors embedded (right). **(G)** Direct comfortable tagging on the Seabream (left) and ability to adapt to different sizes of species due to the interlocking mechanism of the soft bracelet (right).

Supporting Information

Title: Non-invasive featherlight wearable compliant "Marine Skin" – standalone multi-sensory system for deep-sea environment monitoring

*Sohail F. Shaikh[1], Harold F. Mazo-Mantilla[1], Nadeem Qaiser[1], Sherjeel M. Khan[1], Joanna M. Nassar[2], Nathan R. Geraldi[3], Carlos M. Duarte[3], and Muhammad M. Hussain[1]**

[1]mmh Labs, Electrical Engineering, Computer Electrical Mathematical Science and Engineering Division (CEMSE), King Abdullah University of Science and Technology (KAUST), Thuwal 23955-6900, Saudi Arabia.
[2]California Institute of Technology, Pasadena, CA 91125, USA.
[3]Red Sea Research Center (RSRC), Division of Biological and Environmental Sciences and Engineering (BESE), King Abdullah University of Science and Technology (KAUST), Thuwal 23955-6900, Saudi Arabia.

*Corresponding author's e-mail: muhammadmustafa.hussain@kaust.edu.sa

Keywords: marine ecology, flexible systems, non-invasive tag, soft packaging, hybrid integration,

1. Material and Design Optimisation

1.1. Temperature Sensor

Oceanic temperature is relatively stable in response to changes in climates, for example, the change in oceanic temperature is effectively 0.1 °C for 0.6 °C change in global average temperature in the last century. However, the temperature of the seawater varies with the increasing depth (200-1500 m) known as thermocline region, which also has a significant effect on the marine ecosystems at different depths. [1–4] We compare the performance of the temperature sensor with the performance of the commercial temperature sensor integrated circuit (IC) from Sensirion. Commercial temperature sensor IC from Sensirion is attached to next to the fabricated temperature sensor on the wafer for accurate temperature detection. Both the reference and test sensors are subjected to heating from room temperature of 21 °C all the way up to 80 °C using a hot air gun. Initially, both the sensors record the values for room temperature which starts

increasing as the hot air gun is brought closer and closer to the sensor gradually. From **Figure S1**, we can clearly observe that change in resistance of version 2 sensor follows exactly with the reference standard. Instantaneous variations in the resistance change not only suggest that the resolution is high but also the response and recovery times match are at least on par with the status quo if not better.

1.2. Salinity Sensor

Similarly, the salinity of the seawater is fairly constant at the surface and at greater depths (> 800 m) but it varies rapidly in the halocline region (the region of rapid change of salinity, ~ 300 – 1000 m) similar to thermocline region for temperature. Variations in the oceanic salinity have been reported to affect the water cycles and the oceanic circulation. Factors that increase the salinity gradually of the oceanic surface are naturally counterbalanced by the inflow of fresh water from rivers, global ice melting, and precipitation of rainwater.[5,6] Ocean surface salinity is also one of the key parameters in understanding the effects of freshwater intake on the ocean dynamics due to occurrences of 86% evaporation and 78% global precipitation over the ocean. Thus, quantifying temperature and salinity can provide us with the basic understanding of the adaptability, habitat, food habits and growth profiles of the marine species. In addition, the density of seawater varies with the variation in temperature, depth, and the salinity. Variations in the density of water are significantly observed in pycnocline region (~ 200 – 500 m) (a subset of the halocline and thermocline regions) whereas, the density variation saturates at depths beyond 1000 m. [2,5] Conventionally, a salinity sensor is a simple 2 electrode design separated by some distance (2 mm in our first version). To increase the stability and the sensitivity, we have modified the design to interdigitated electrode pattern and hence observed more than ~625% increase in the sensitivity with stable and robust performance (**Figure S2**). We also observed ~135% increment in the sensitivity due to change of material from Au to Cu (**Figure S2b**), however, an effect has

been neglected due to corrosive nature of Cu which can degrade the performance of exposed salinity sensor underwater.

1.3. Pressure Sensor

The underwater pressure of the oceanic environment is directly related to the height of the water ($\boldsymbol{P = \rho \cdot h \cdot g}$) where $\boldsymbol{P}$ is the hydrostatic pressure, $\boldsymbol{\rho}$ is the density of water, $\boldsymbol{g}$- acceleration due to gravity, and $\boldsymbol{h}$-represents the height of water. The total pressure exerted ($\boldsymbol{P_{total}}$) on any object underwater is the combination of partial hydrostatic pressure $\boldsymbol{P}$ and the atmospheric pressure ($\boldsymbol{P_0}$), ($\boldsymbol{P_{total} = P + P_0}$) at the sea level which measures 14 psi for each atmospheric pressure. Conventional pressure sensors have high sensitivity with a caveat of low operating range, which restricts the usage in the marine sensors. Hence, we have designed our depth sensor based on a parallel plate capacitance principle where the capacitance varies linearly with the increasing depth with extremely good sensitivity and instantaneously. We chose PDMS due to its compressive nature as a dielectric material for capacitive pressure monitoring underwater. Due to its inherent compressive nature, we could use it as a dielectric material that can change the thickness on pressure application and hence the capacitance change is detected in response to the pressure. PDMS is prepared by mixing the elastomer to curing agent in the ratio of (10:1) is cured mostly at 90 °C for 60 minutes. However, altering the mixing ratio and curing temperature modifies the compressibility and elasticity of PDMS. To improve the compressibility of the dielectric layer, we modified the PDMS elastomer to curing agent mixture during preparation. Increase in elastomer ratio (12:1) from (10:1) and curing at a relatively low temperature (60 °C) resulted in increased compressibility implying increased sensitivity. Also, the thickness of the dielectric layer plays an important role in having increasing the detection range of the pressure (or depth). We have observed higher sensitivity for 1:12 composition of PDMS (**Figure S3a**) whereas similar increment was observed for thickness of 50 μm (**Figure S3b**). Our material choices and the

optimisation has increased the operating range up to 2 km which was only restricted due to non-availability of the tool that can simulate higher pressure than equivalent to 2 km.

For depth measurements at a high-pressure environment, we used a hydraulic pressure simulation tool available in the lab. The tool has the capabilities to control the applied pressure in the chamber filled with water up to a maximum pressure of 3000 psi, which is equivalent to a depth of 2000 m. However, the recommended maximum value for applied pressure was 2300 psi for the equipment restricting our measurements to a maximum pressure equivalent to a depth of 1500 m (**Figure S4**). The experimental setup is shown in **Figure S4b** in which the sensor is immersed in a closed metallic vessel (~70 cm tall with an internal diameter of 15 cm) with thermal insulation from outside, connected to a digital and manual pressure control system. The simulation tool is a custom designed set-up that has 3 different components: pressure and temperature controller, hydraulic pump, and the chamber. The hydraulic pump is mainly for applying manual pressure (Figure S4b right inset). The applied pressure can be calibrated or readout using an analog dead weight measurement system (Ametek test & calibration instruments) or digital tools (Digiquartz Portable Standard from Paroscientific Inc.). The steel vessel that is filled with the seawater also has waterproof connectors that can be connected to other tools like Oscilloscope, function generator or any other electronic instrument. We started with digitally controlling the pressure applied through a small hydraulic hand-pump, however, observed a lot of noise in the recording of the signal. This noise was figured to be originating from the electrical interference of the connections of a digital control system to the steel vessel. We switched to manual control mode and applied pressure in an incremental way up to 1500 m with a step size of 30 m (~43 psi). Real-time variation in capacitance of pressure/depth sensor with respect to the applied changing pressure has been plotted in Figure S3a. It can be seen that the sensor exhibits a linear relationship to the

change in depth of the water with extremely fast response time. An incremental increase in the capacitance with the corresponding step increase in applied pressure appears to be constant throughout the entire range. From this response, it can be conferred that sensor performance neither degrade nor reach a saturation in the value, thereby can withstand the pressure of water higher than the depths of 2 km. One can observer oscillations in the capacitance change from **Figure S4**, with incremental pressure. These oscillations are arising from the decrease in the pressure during manual application of pressure, and hence the hydraulic pressure drops initially then ramps up to the desired values. These oscillations to the variations in the pressure experienced during the step increment confirm high sensitivity and the resolution of the depth sensor.

2. Rugged Performance Testing

2.1. Cyclic Bending Tests

For the reliability of the Marine Skin, it is important to study the effect of the harsh environmental parameters that it may experience. The two important parameters are high salinity exposure for extended periods (multiple weeks) and no degradation in the performance due to physical deformations. First, the ruggedness of the depth sensors and integrity of packaging were tested by subjecting the fabricated Marine Skin to a large number of bending cycles with the bending radius of 1 mm. Depth measurements in the lab environment are carried out after 100, 500, 1000, 2500, and 10^4 bending cycles (**Supplementary Video S1**). Real-time variations in the capacitance while submerging in the water in steps of 10 cm each plotted in **Figure S5** where the change in each step is consistent with the only variation due to the manual handling error in maintaining constant step height increment. The sharp increase in the capacitance occurs as soon as the sensor is immersed in water from the air. To confirm the reliability for the ruggedness over different cycles, hysteresis tests are performed where measurements are recorded at specific depths during increasing depths (submerging) and decreasing depths (rising up) of water. **Figure S6**

illustrates excellent hysteresis characteristics of the sensors the variation in depth, nevertheless, the variations in the hysteresis can also be attributed to variations occurring due to manual handling.

2.2. Prolonged Exposure to Saline Environment

Similarly, the packaging integrity is validated from the prolonged exposure of high salinity (41 PSU) Red Seawater on the sensors. We immersed the packaged Marine Skin platform in the seawater and measured the performance after 1 day, 3 days, 7 days, 15 days and 28 days to evaluate the integrity of packaging. The real-time change in the capacitance with increasing depth of the water is acquired (**Figure S7**) for these different scenarios, which show no degradation in terms of saturation or sensitivity. Thus, we can conclude that the integrity of packaging and the reliability of the sensors makes the Marine Skin platform an extremely robust, flexible, and highly lightweight solution for marine environmental monitoring.

3. Attachment Strategies and Wearable Bracelet Design

3.1. Attachment on Large Species

The tagging of the marine species has always been a non-invasive method involving incisions through skin, tissues, usage of metallic and plastic anchors inserted in the skin. Invasive method of attachment can lead to the injury of the species, which not only introduces great discomfort to the tagged individual but also can affect their normal movements and behavior. Thus, the requirement of 2% body weight of the bio-loggers, flexibility and non-invasive nature of the devices are under focus. Our focus was on making a flexible standalone system that can adhere to all these norms in addition to having a completely non-invasive tagging mechanism. In past, Marine Skin version 1, was tested for its flexibility and non-invasive method attachment on tiger shark, wobbegong shark, and stingray (**Figure 7**). We mounted the sensors on a cylindrical CAN

host attached to a steel clamp that was attached to the dorsal fin of the shark. This method can only be applicable to large species with the dorsal fin acting as an anchor for the sensing system. For other species with comparatively smoother and mucous skin or smaller sized animals, we needed to use other techniques. Superglue can be used on the species with hard shells (turtles, crab etc.) whereas as dental/surgical glue was tested on a wobbegong and Stingray (**Supplementary Video S3**). The hydrodynamic forces due to the stream of water detach the sensors from the body of the animal. Not only the water stream but also this glue is dissolvable in water in 48 hours making this method unsuitable for long-term deployment.

3.2. Wearable Bracelet Design

We designed a unique strategy of making a soft elastic wearable jacket (bracelet) like structure to host the sensors made from the same material. The wearable gadget can be wrapped around the species and its strong locking mechanism can prevent it from detachment due to water stream itself. We made 3D printed molds for replicating the wearable modules, followed by pouring PDMS to cure at 60 °C for an hour. This cured wearable jacket design embedded with the sensory platform can be easily peeled from the mold (**Figure S9**). In the initial design, we used the locking mechanism of soft-pins and the holes made from the same PDMS material (**Figure S9c**). However, the design of the soft pins was not strong enough to withstand the stream pressure, in addition, the adhesive strength was not sufficient to hold the jacket on the skin. We modified the design to incorporate a 3D printed pin structure for increasing the strength of the locking mechanism. These 3D printed mushroom pins provide excellent strength and hence the successful attachment on barramundi and seabream fishes can be seen in **video S4 and S5**. Dental adhesive can be used on the inner lining of the soft wearable bracelet to reduce the friction between the

elastic soft material and the skin and hence reducing the minuscule probability of injury due to this soft bracelet.

REFERENCES

[1] J. B. C. Jackson, M. X. Kirby, W. H. Berger, K. A. Bjorndal, L. W. Botsford, B. J. Bourque, R. H. Bradbury, R. Cooke, J. Erlandson, J. A. Estes, T. P. Hughes, S. Kidwell, C. B. Lange, H. S. Lenihan, J. M. Pandolfi, C. H. Peterson, R. S. Steneck, M. J. Tegner, R. R. Warner, *Science (80-.).* **2001**, *293*, 629.

[2] USEPA, "Climate Change Indicators: Stream Temperature," can be found under https://www.epa.gov/climate-indicators/climate-change-indicators-sea-surface-temperature, **2016**.

[3] S. C. Doney, M. Ruckelshaus, J. Emmett Duffy, J. P. Barry, F. Chan, C. A. English, H. M. Galindo, J. M. Grebmeier, A. B. Hollowed, N. Knowlton, J. Polovina, N. N. Rabalais, W. J. Sydeman, L. D. Talley, *Ann. Rev. Mar. Sci.* **2012**, *4*, 11.

[4] J. H. Koo, D. C. Kim, H. J. Shim, T. H. Kim, D. H. Kim, *Adv. Funct. Mater.* **2018**, DOI 10.1002/adfm.201801834.

[5] "Salinity | Science Mission Directorate," can be found under https://science.nasa.gov/earth-science/oceanography/physical-ocean/salinity, **n.d.** in *Int. Geophys.*, **1994**, pp. 171–203.

SUPPORTING FIGURES

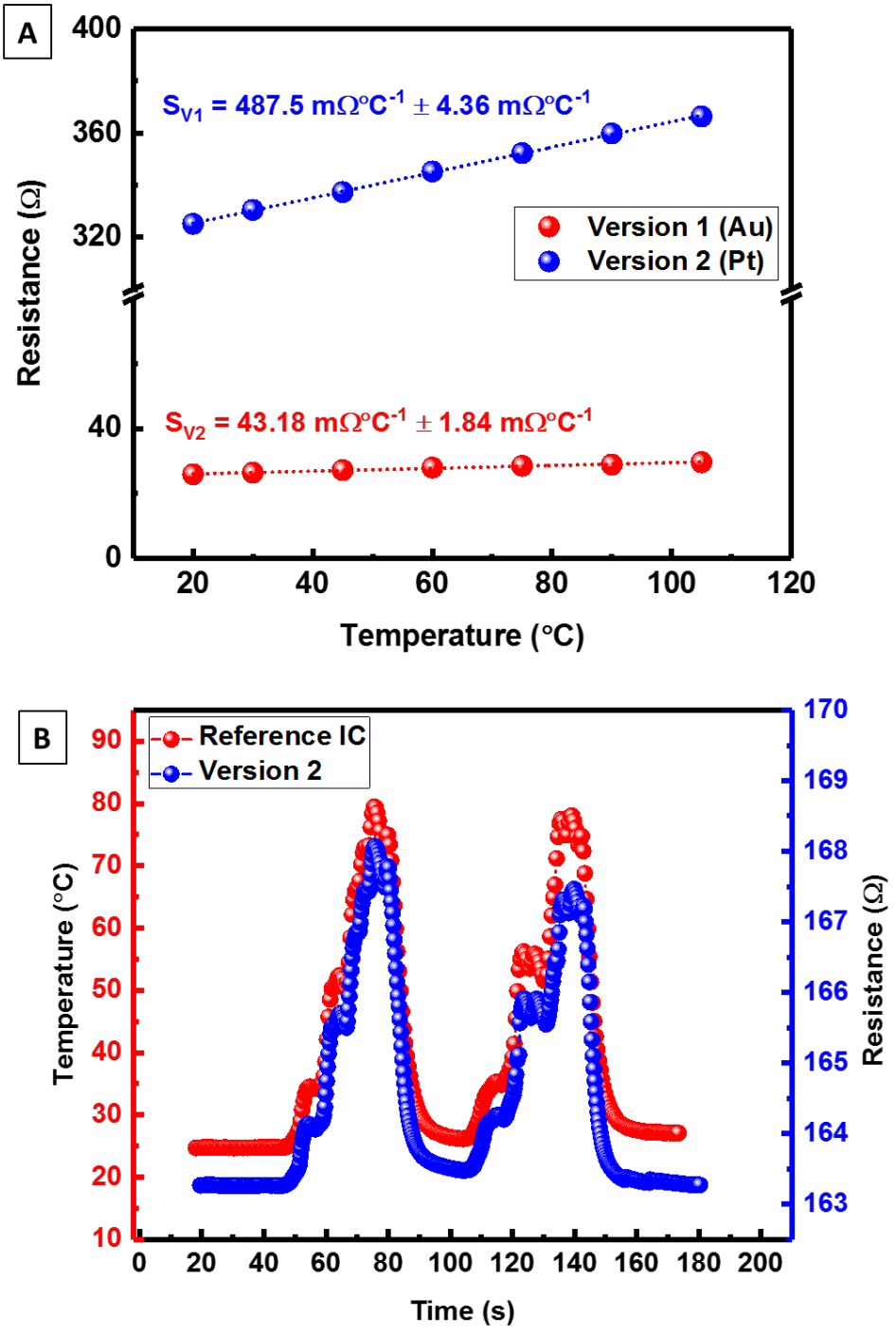

Figure S1: Comparison of the performance of (A) version 1 and version 2 temperature sensor for material choice and improved sensitivity, and (B)Version 2 comparison and calibration with the commercial temperature sensor IC from Sensirion. Fabricated sensors changes the resistance corresponding to the temperature with the response exactly following the reference sensor.

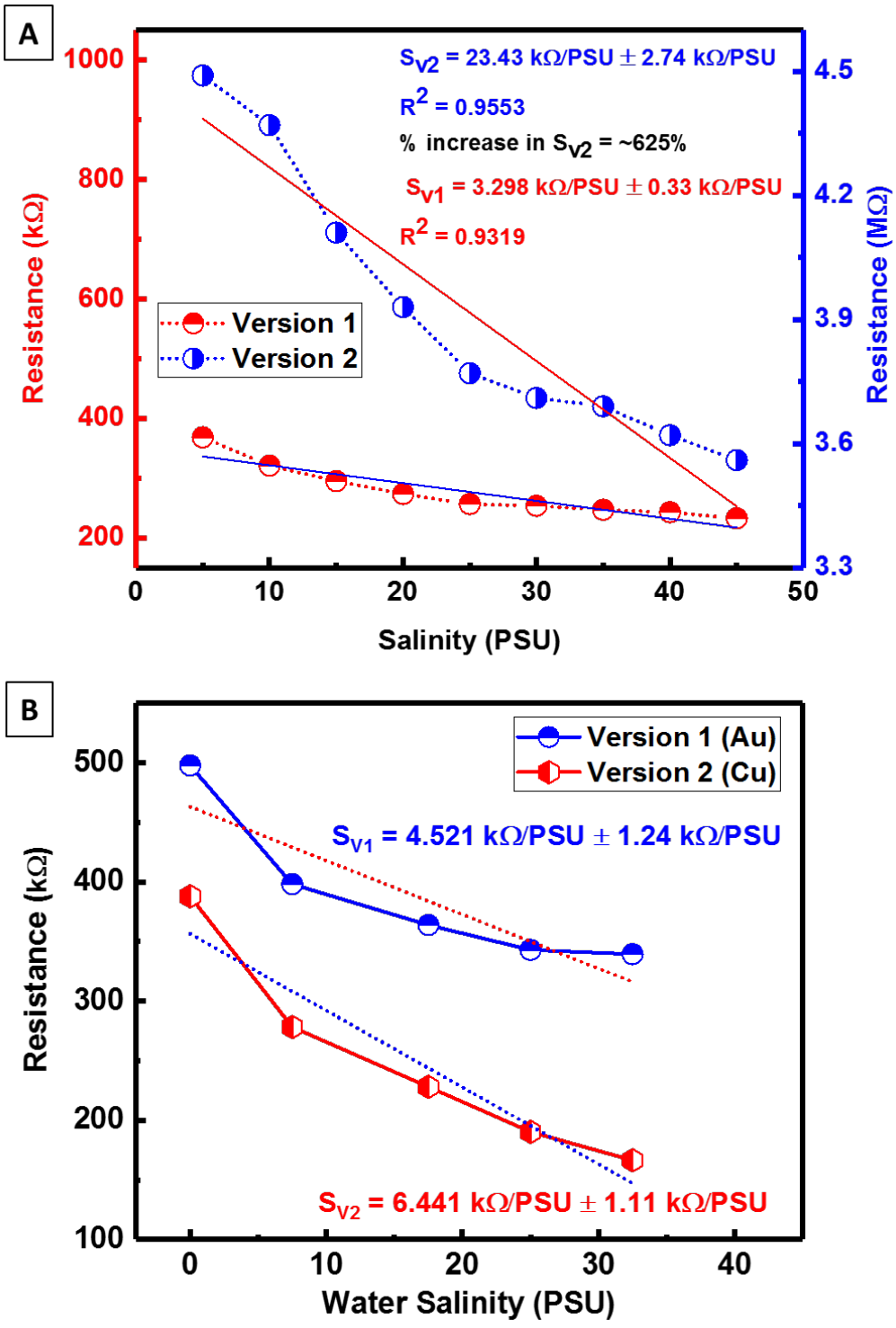

Figure S2: Comparison of the performance of (A) previous version and present version water salinity sensor for improved sensitivity by modified design, and (B) Present version comparison for two different material choices of Au and Cu. An increase of ~625% sensitivity is observed due to design modification, while increase in sensitivity has been neglected.

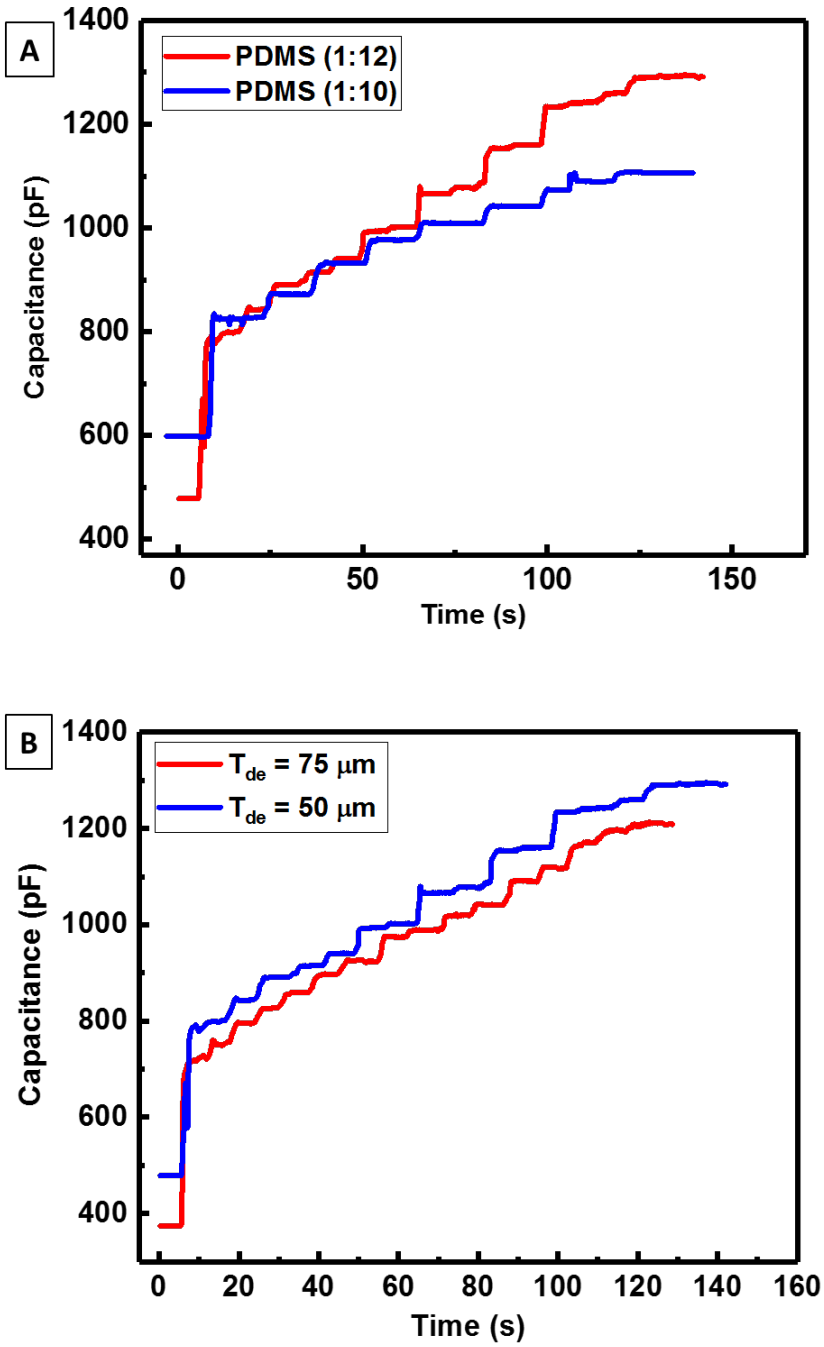

Figure S3: Dielectric material optimisation for pressure increasing the pressure sensitivity and the range of depths that can be measured. (A) Effect of the variation in the mixing ratio of PDMS elastomer to curing agent, with (12:1) ratio showing higher sensitivity due to increased compressibility. (B) Effect of dielectric thickness variation on sensitivity and absolute values, optimum thickness is 50 µm.

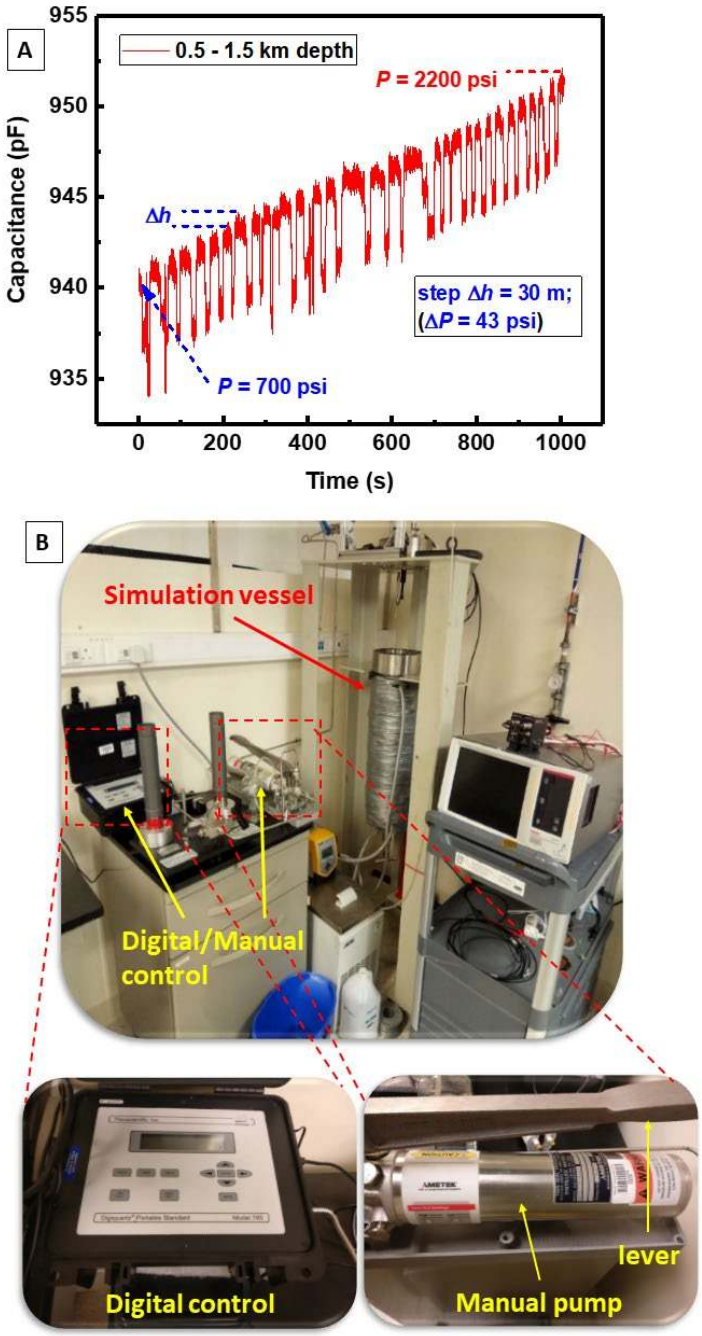

Figure S4: Harsh marine environment real-time pressure recording using version 2 Marine Skin platform, (A) demonstrating linear increment with the increased pressure, high sensitivity, resolution and fast response time by observed oscillations due to manual handling. (B) Experimental setup for the high-pressure simulation and testing in the central labs (inset shows magnified images of digital control for temperature and pressure (left black box) and manual control unit for pressure using a hydraulic pump pumped using a manual handheld lever. A dead weight analog reading is also visible that looks like poles in B.

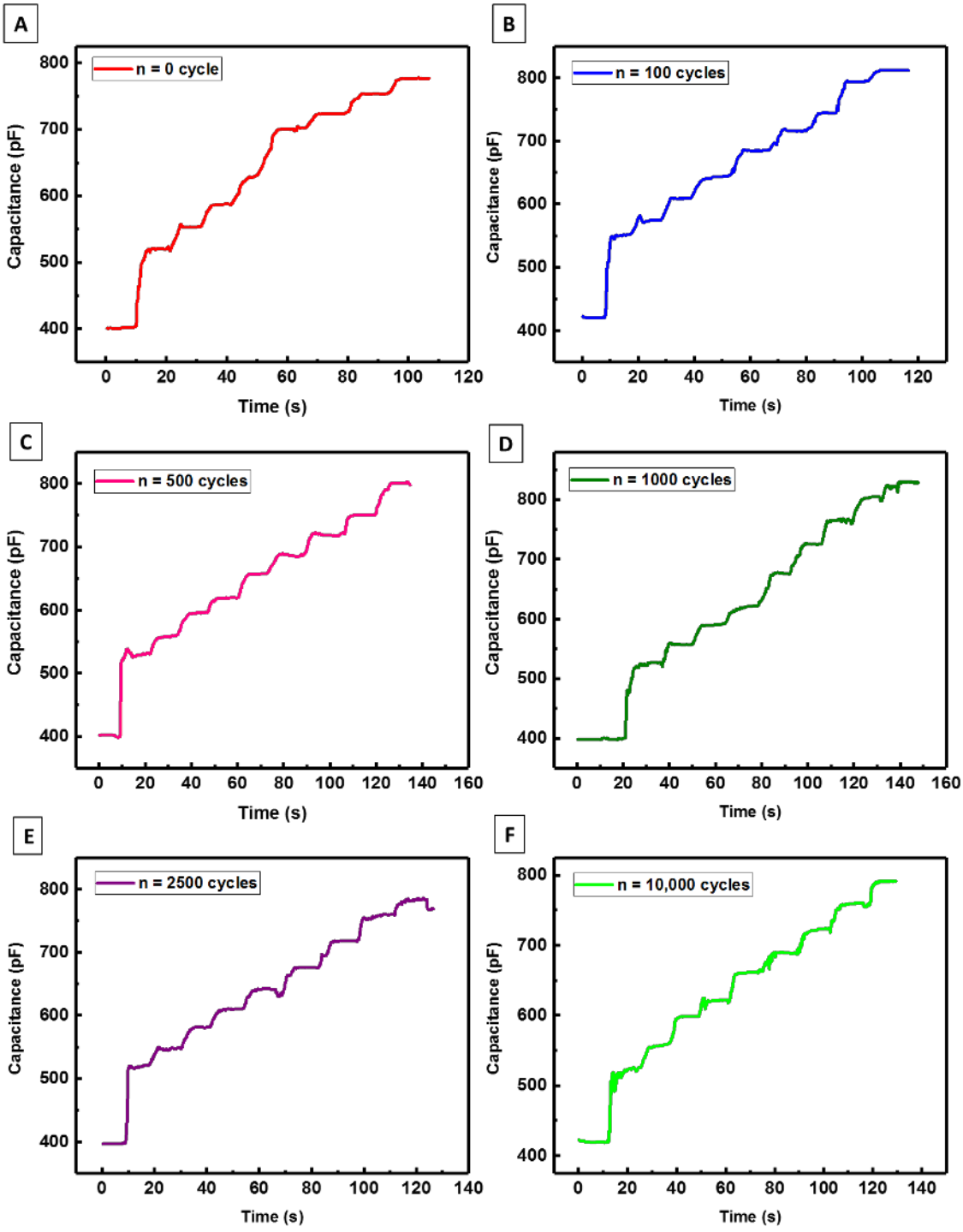

Figure S5: Real-time depth measurements over multiple bending cycles. Measurements are recorded after subjecting sensor to the multiple bending cycles (A)-(F) from 0 to 10,000 cycles. Real-time measurements of change in capacitance with increasing pressure (due to incremental depth) are observed with similar sensitivities.

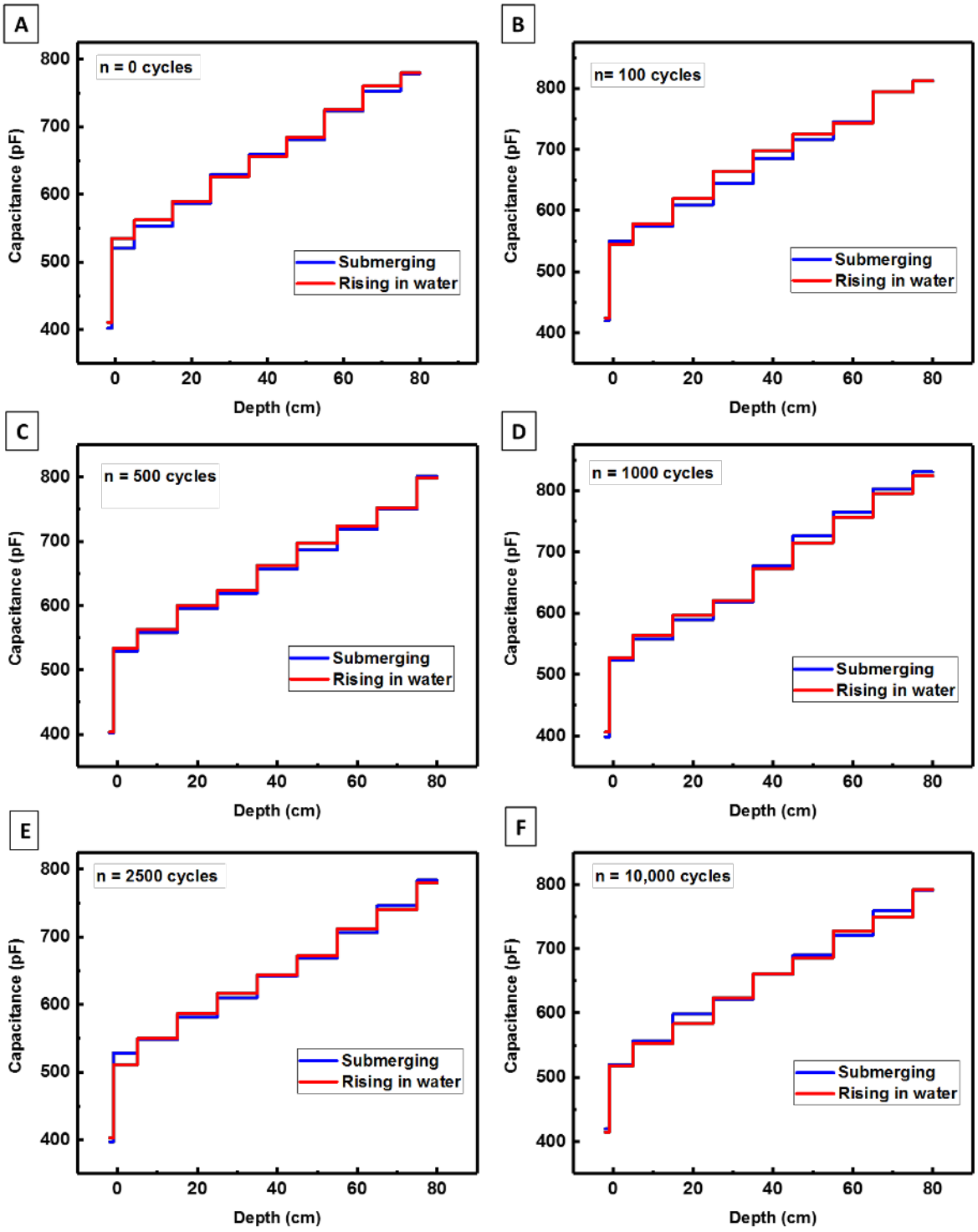

Figure S6: Robustness of the pressure sensor characterized for the pressure sensor when subjected to extreme bending cycle test of (1 mm bending radii) (A) - (F) with 0, 100, 500, 1000, 2500, and 10 thousand cycles respectively. Discrete measurements are plotted at step heights of ~10 cm for observing the hysteresis during submerging and rising from the water in the acrylic tank.

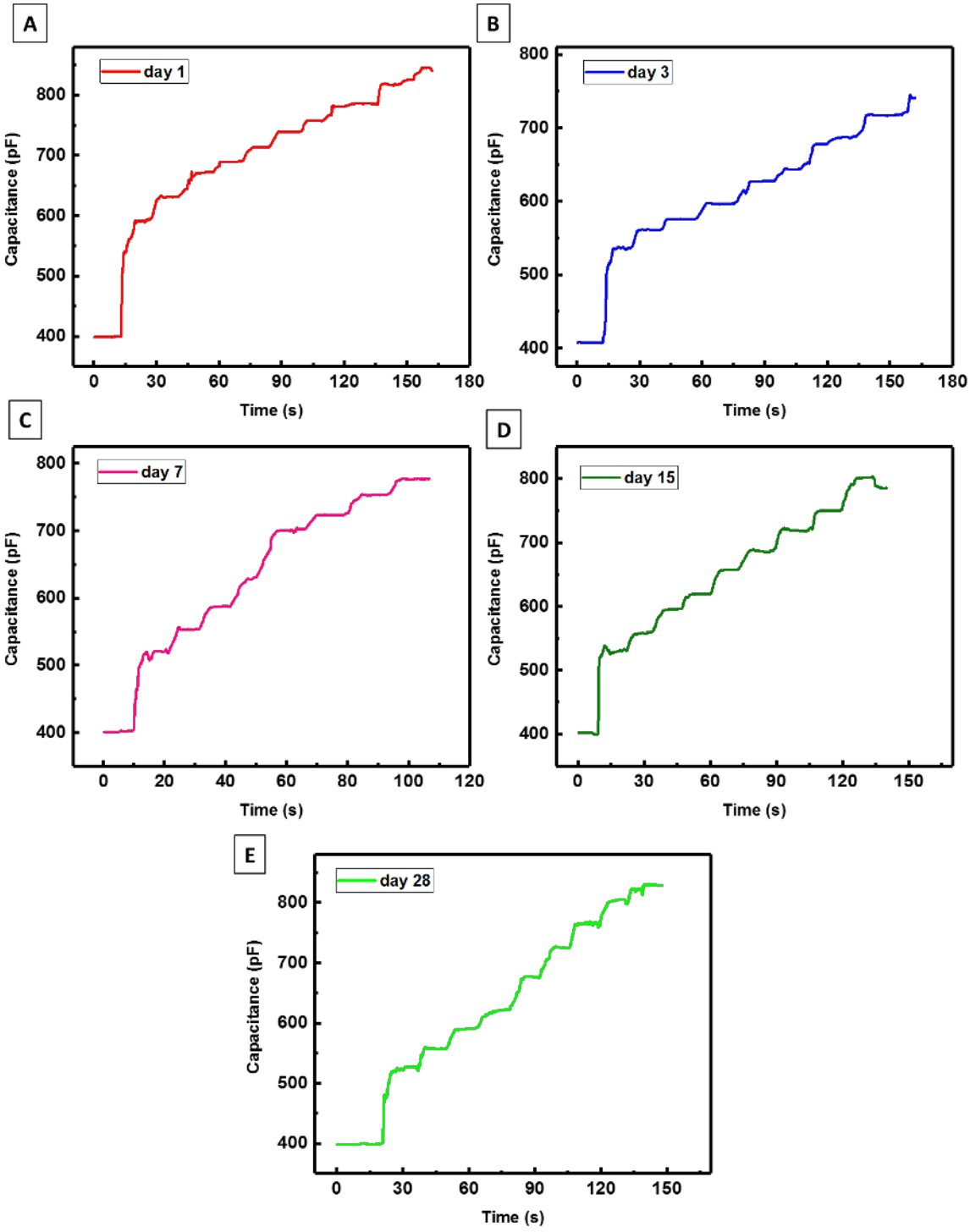

Figure S7: Real-time depth measurements against the time while submerging the sensors in the seawater in steps of 10 cm to observe the effect of prolonged exposure to saline water. (A) – (E) Devices were characterized after 1 day, 3 day, 7, 15, and 28 days of immersion in the Red sea water (41 PSU) and has observed no significant change in performance.

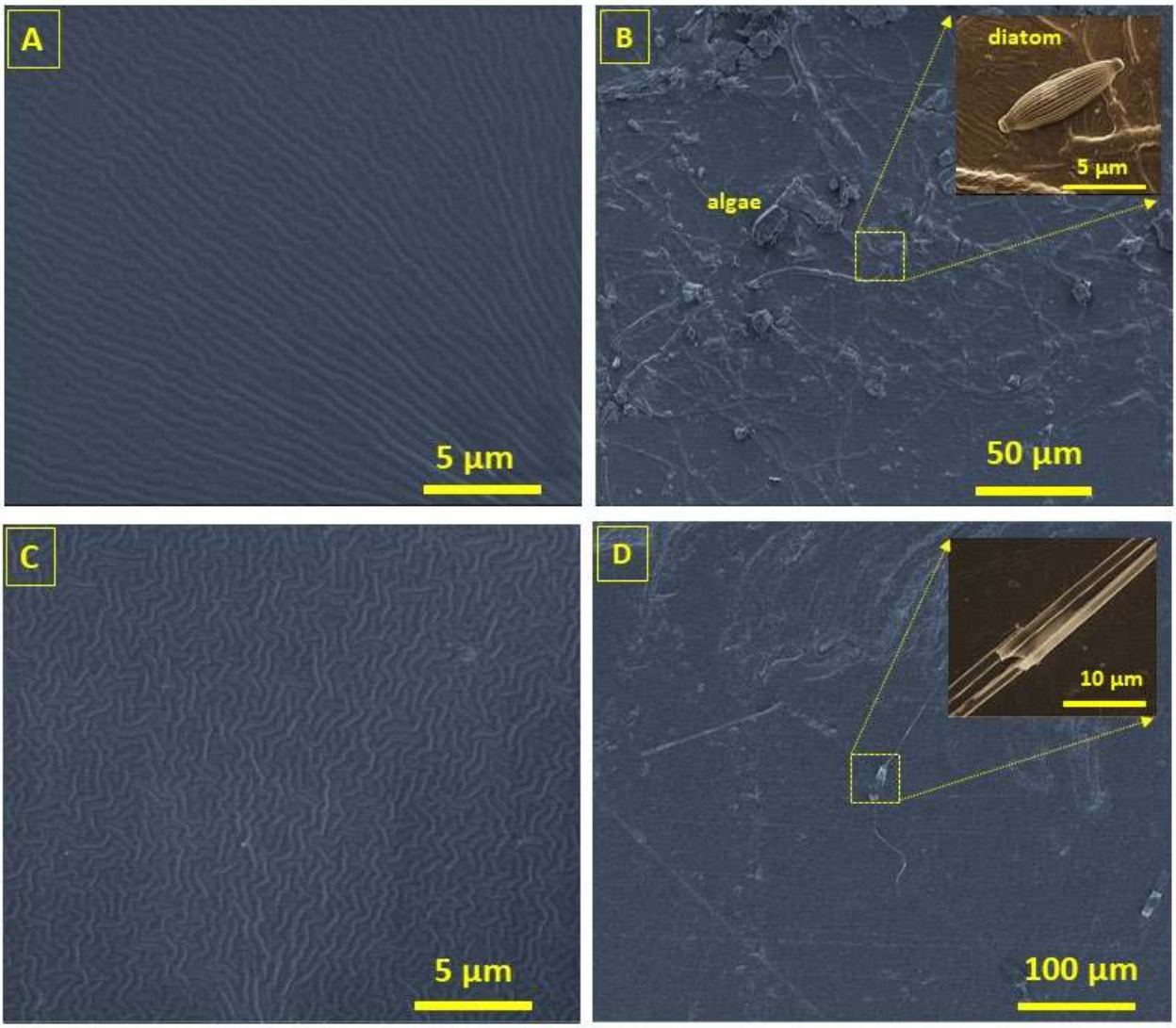

Figure S8: Scanning electron microscopic (SEM) images of the soft-polymeric encapsualted packaging for studying the biofouling effect. Samples has been submerged in the Red sea water for 6 weeks and then a standrad process was followed to fix any kind of biological traces on the sample followed by acquiring the SEM images. SEM of blanket PDMS showing different textures (A) before and (C) after O_2 plasma treatment for samples to be immersed in water. (B) sample 1 showing development of algea and salt accumulation with a few traces of diatoms (inset) after 6 weeks of constant sumbersion in the Red seawater. And (D) the significant reduction in the biofouling development due to treatment and weak adhesion forces of the biofouling organisms that are self-released by drag forces within the water stream.

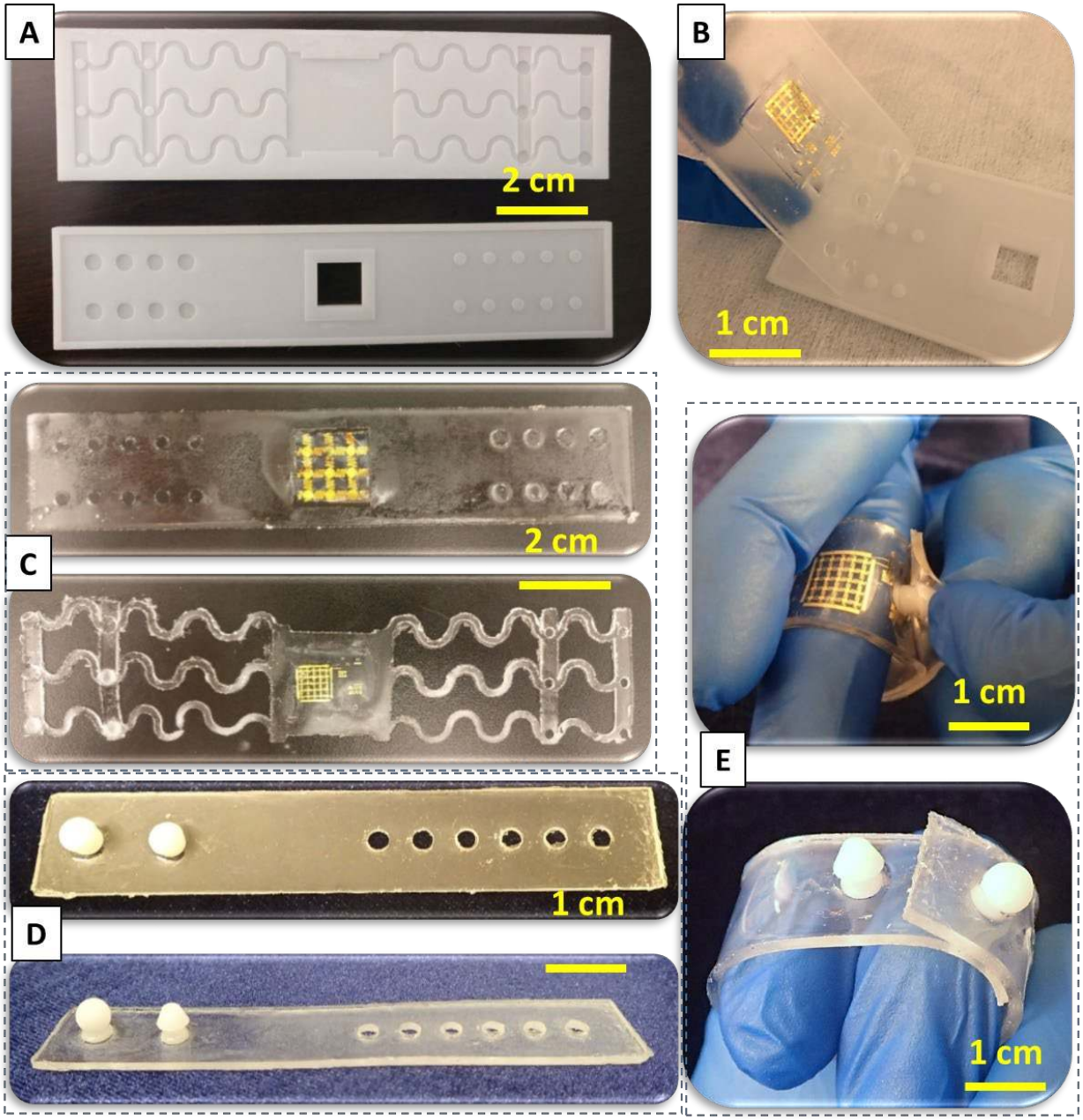

Figure S9: (A) 3D printed mold designs for multiple wearable bracelet. (B) Easy peeling-off of the flexible and stretchable bracelet from the 3D mold, (C) two designs having Marine Skin embedded within the bracelet with soft-mushroom pins to hold. Serpentine structures (bottom) can provide more breathability for animal and stretchability to the bracelet. (D) Modified bracelet design with 3D printed mushroom pins (spherical and trapezoidal shape) to improve inter-locking mechanism. (E) Increased inter-locking strength due to the incorporation of 3D printed mushroom pins has little effect on the flexibility.

Supplementary Video 1

Supplementary Video 2

Click here to access/download

Supporting Information

Video S2.wmv

Supplementary Video 3

Click here to access/download

Supporting Information

Video S3.wmv

Supplementary Video 4

Click here to access/download

Supporting Information

Video S4.wmv

Supplementary Video 5

Click here to access/download

Supporting Information

Video S5.wmv